Acknowledgment

The authors thank the staff at the Mayo Clinic Alzheimer's Disease Research Center for assistance in evaluating the subjects and the members of the PPND kindred for their participation.

From the Departments of Neurology (A.R.F., B.F.B.) and Diagnostic Radiology (C.R.J.), Mayo Clinic College of Medicine, Rochester, MN, and Department of Neurology (Z.K.W.), Mayo Clinic College of Medicine, Jacksonville, FL.

Supported by grants AG16574, AG11378, and AG07216 from the National Institute on Aging and the Robert H. and Clarice Smith and Abigail Van Buren Alzheimer's Disease Research Program of the Mayo Foundation.

Disclosure: The authors report no conflicts of interest.

Received Jun. 14, 2006. Accepted in final form November 1, 2006.

Address correspondence and reprint requests to Dr. Z.K. Wszolek, Mayo Clinic Jacksonville, 4500 San Pablo Rd., Jacksonville, FL 32224; e-mail: wszolek.zbigniew@mayo.edu

References

1. Wszolek ZK, Pfeiffer RF, Bhatt MH, et al. Rapidly progressive autosomal dominant parkinsonism and dementia with pallido-ponto-nigral degeneration. Ann Neurol 1992;32:312–320.
2. Reed LA, Schmidt ML, Wszolek ZK, et al. The neuropathology of a chromosome 17-linked autosomal dominant parkinsonism and dementia ("pallido-ponto-nigral degeneration"). J Neuropathol Exp Neurol 1998; 57:588–601.
3. Cordes M, Wszolek ZK, Calne DB, Rodnitzky RL, Pfeiffer RF. Magnetic resonance imaging studies in rapidly progressive autosomal dominant parkinsonism and dementia with pallido-ponto-nigral degeneration. Neurodegeneration 1992;1:217–224.
4. Clark LN, Poorkaj P, Wszolek ZK, et al. Pathogenic implications of mutations in the tau gene in pallido-ponto-nigral degeneration and related neurodegenerative disorders linked to chromosome 17. Proc Natl Acad Sci USA 1998;95:13103–13107.
5. Pal PK, Wszolek ZK, Kishore A, et al. Positron emission tomography in pallido-ponto-nigral degeneration (PPND) family (frontotemporal dementia with parkinsonism linked to chromosome 17 and point mutation in tau gene). Parkinsonism Relat Disord 2001;7:81–88.

Vocal cord paralysis in myasthenia gravis with anti-MuSK antibodies

K. Hara, MD, PhD; T. Mashima, MD; A. Matsuda, MD; K. Tanaka, MD, PhD; M. Tomita, MD, PhD; H. Shiraishi, MD, PhD; M. Motomura, MD, PhD; and M. Nishizawa, MD, PhD

About 20% of patients with generalized myasthenia gravis (MG) have undetectable serum antibodies to the nicotinic acetylcholine receptor (AChR). These patients are referred to as having seronegative MG. Recently, it has been demonstrated that about 50% of patients with generalized seronegative MG have antibodies to the surface membrane enzyme muscle-specific tyrosine kinase (MuSK) in Caucasian populations and a high frequency of respiratory crises.[1] Here, we report a case of MG with anti-MuSK antibodies presenting with vocal cord paralysis, facial muscle weakness, and bulbar palsy.

Case report. A 56-year-old man showed mild upper limb muscle weakness and fatigue on swallowing and chewing that worsened at the end of days in April 2000. He was admitted to our hospital in February 2001. Neurologic examination revealed mild muscle weakness and atrophy of his proximal muscles in the neck, shoulder, upper arm, and thigh. Nasal voice and dysphagia and facial muscle weakness were also observed, There was no ptosis or diplopia. Although repetitive nerve stimulation (RNS) showed a decrementing response in abductor digiti minimi and orbicularis oculi muscles, anti-AChR antibodies were not detected and the edrophonium (anticholinesterase) test was negative. CT scan of his thorax showed no thymoma. As we observed obvious muscle atrophy in his proximal muscles without fluctuation of muscle weakness, we thought a myopathy with myasthenic features[2] was likely present. The thyroid profile demonstrated elevated levels of anti-thyroglobulin antibodies (676.0 U/mL; normal range <0.3 U/mL), anti-thyroid peroxidase antibodies (812 U/mL; normal range <0.3 U/mL), and thyroid-stimulating hormone (43.74 μIU/mL; normal range 0.6 to 4.1 μIU/mL) with a low level of free thyroxine (0.5 ng/dL; normal range 0.9 to 1.6 ng/dL). Thyroid anti-microsomal antibodies showed an elevated titer of 1:6,400 (normal range <60). Thus, a diagnosis of hypothyroid myopathy caused by autoimmune chronic thyroiditis was made, and thyroid hormone replacement therapy resulted in improvement in proximal muscle weakness, whereas bulbar palsy and facial muscle weakness did not improve satisfactorily.

On June 9, 2005, the patient presented with a 3-month history of exertional dyspnea and stridor, which worsened at the end of days. Arterial blood gas analysis showed normal results in room air: pH, 7.406; P_aO_2, 92.7 mm Hg; and P_aCO_2, 43.8 mm Hg. However, the pulmonary function test showed a substantial reduction in ventilatory muscle strength; vital capacity (VC) was 2.5 L, and %VC was 71.2%. Fiberoptic laryngoscopy revealed that his vocal cords were located in the paramedian position and the abduction of the vocal cords in inspiration was limited (figure, A). Vocal cord movement did not change after an IV injection of edrophonium. Tracheostomy was performed on June 15, 2005, although the etiology of his vocal cord paralysis remained unknown. We considered the fluctuation of stridor and the decrementing response on RNS as clues to the etiology. We investigated anti-MuSK antibodies and detected an elevated anti-MuSK antibody (6.25 nmol/L; normal range <0.05 nmol/L). Oral prednisolone therapy was initiated on October 27, 2005, leading to improvement of bulbar palsy and facial weakness. Fiberoptic laryngoscopy performed on December 20, 2005, also revealed an opening in the airway and improvement of vocal cord paralysis (figure, B). After more than 6 months of follow-up and continued treatment for MG, the patient continues to require tracheostomy, because his vocal cord paralysis persists.

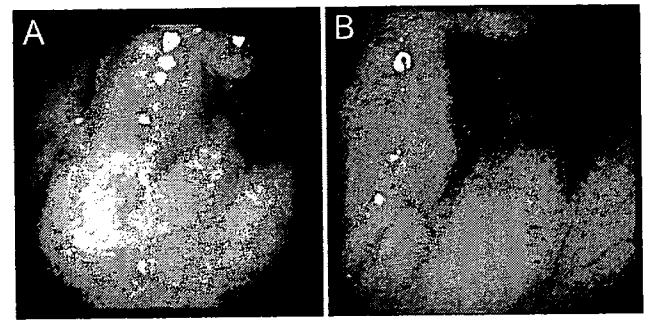

Figure. Fiberoptic laryngoscopic findings of maximal abducent position of vocal cords. (A) There was a limitation of abduction of the vocal cords before prednisolone treatment. (B) An opening in the airway and improvement of vocal cord paralysis were observed after treatment.

Discussion. Vocal cord paralysis associated with MG has been reported including cases with anti-AChR antibodies[3-5] and seronegative MG.[6,7] However, it is interesting that this patient with MG, presenting with vocal cord paralysis after a 5-year history of fatigue on swallowing and chewing, had anti-MuSK antibodies. Thus, vocal cord paralysis is considered a new clinical presentation of MG with anti-MuSK antibodies. Furthermore, MG can show respiratory crisis due to vocal cord paralysis without severe respiratory muscle paralysis in previously reported patients[3-7] and this patient. Although the edrophonium test was positive in all of those reported patients with MG with vocal cord paralysis, it was negative in our patient, which delayed the diagnosis of MG. As the effect of edrophonium is negative in 30% of MG with anti-MuSK antibodies,[1] there is the possibility of MG with anti-MuSK antibodies, even if the edrophonium test is negative.

Because it is difficult to make a diagnosis of MG in seronegative MG with only stridor as a initial symptom,[6,7] it might be useful to investigate the anti-MuSK antibodies in those patients, particularly in patients with bulbar palsy and facial weakness.

From the Department of Neurology (K.H., T.M., A.M., K.T., M.N.), Brain Research Institute, and Department of Otolaryngology (M.T.), Faculty of Medicine, Niigata University, and First Department of Internal Medicine

(H.S., M.M.), Graduate School of Biomedical Sciences, Nagasaki University, Japan.

Disclosure: The authors report no conflicts of interest.

Received July 4, 2006. Accepted in final form November 2, 2006.

Address correspondence and reprint requests to Dr. M. Nishizawa, Department of Neurology, Brain Research Institute, Niigata University, 1-757 Asahi-machi-dori, Niigata, 951-8585, Japan; e-mail: nishi@bri.niigata-u.ac.jp

References

1. Evoli A, Tonali PA, Padua L, et al. Clinical correlates with anti-MuSK antibodies in generalized seronegative myasthenia gravis. Brain 2003; 126:2304–2311.
2. Nishida Y, Kobayashi T, Machi M, et al. Congenital myopathy with myasthenic features and congenital cataract in two siblings. J Neurol 1989;236:161–163.
3. Schmidt-Nowara WW, Marder EJ, Feil PA. Respiratory failure in myasthenia gravis due to vocal cord paresis. Arch Neurol 1984;41: 567–568.
4. Fairley JW, Hughes M. Acute stridor due to bilateral vocal fold paralysis as a presenting sign of myasthenia gravis. J Laryngol Otol 1992;106: 737–738.
5. Hanson JA, Lueck CJ, Thomas DJ. Myasthenia gravis presenting with stridor. Thorax 1996;51:108–109.
6. Abul Matin M, Alam K, O'Driscoll K, Murphy PJ. Acute inspiratory stridor: a presentation of myasthenia gravis. J Laryngol Otol 1999;113: 1114–1115.
7. Osei-Lah V, O'Reilly BJ, Capildeo R. Bilateral abductor vocal cord paralysis due to myasthenia gravis. J Laryngol Otol 1999;113:678–679.

Steroid dementia: A follow-up

Oliver Sacks, MD, FRCP; and Melanie Shulman, MD

We offer a follow-up report on the patient described in our brief communication, "Steroid dementia: an overlooked diagnosis."[1]

We described how Mr. K originally developed a mixed picture of psychosis and an Alzheimer-like dementia in the summer of 2001, apparently in consequence of the steroids he was taking. His psychosis promptly cleared when the steroids were stopped, and his intellectual status improved greatly, although some evidence of intellectual and executive compromise remained. It was still unclear, when we last saw Mr. K. (in September 2003), whether there might have been a core of neurodegenerative disease in addition to the seemingly reversible steroid dementia.

We have recently (June 2006) re-examined Mr. K. He continues, at age 76, to travel extensively and to work fulltime as an international businessman. He is able to manage all of his financial dealings independently. He scored 30 of 30 on a Mini-Mental State Examination and had a digit span of 8 digits forward and 6 backward. He scored 56 of 60 on the Boston Naming Test.[2] He was able to name 21 animals in 60 seconds (albeit with two perseverations) and did alphanumeric sequencing rapidly (40 seconds) and without error. Immediate and delayed recall, language comprehension of syntax–complex material, visual constructions, etc., were equally intact.

This robust performance on all cognitive fronts, 5 years after he was considered to have Alzheimer disease, is inconsistent with such a diagnosis and seems to confirm our impression that his months-long dementia in 2001 was solely a consequence of the steroids he was taking.

From the Albert Einstein College of Medicine (O.S.) and NYU School of Medicine (O.S., M.S.), New York.

Disclosure: The authors report no conflicts of interest.

Received August 11, 2006. Accepted in final form November 6, 2006.

Address correspondence and reprint requests to Dr. O. Sacks, 2 Horatio St., 3G, New York, NY 10014; e-mail: mail@oliversacks.com

References

1. Sacks O, Shulman M. Steroid dementia: an overlooked diagnosis. Neurology 2005;64:707–709.
2. Kaplan EF, Goodglass H, Weintraub S. The Boston Naming Test. 2nd ed. Philadelphia: Lea and Febiger, 1983.

JOURNAL OF CLINICAL MICROBIOLOGY, Jan. 2007, p. 112–120 Vol. 45, No. 1
0095-1137/07/$08.00+0 doi:10.1128/JCM.00718-06

Genetic Diversity of Coxsackievirus A16 Associated with Hand, Foot, and Mouth Disease Epidemics in Japan from 1983 to 2003[▽]

Mitsuaki Hosoya,[1]* Yukihiko Kawasaki,[1] Masatoki Sato,[1] Ken Honzumi,[1] Akio Hayashi,[2] Toyomasa Hiroshima,[2] Hiroaki Ishiko,[2] Kazuo Kato,[3] and Hitoshi Suzuki[1]

Department of Pediatrics, Fukushima Medical University School of Medicine, Fukushima 960-1295,[1] Research and Development Department, Mitsubishi Kagaku Bio-Clinical Laboratories, Inc., Tokyo 174-8555,[2] and Fukushima Institute for Public Health, Fukushima 960-8560,[3] Japan

Received 5 April 2006/Returned for modification 5 July 2006/Accepted 21 October 2006

To clarify the chronologic genetic diversity of coxsackievirus A16 (CV-A16) strains associated with hand, foot, and mouth disease (HFMD) epidemics in a restricted area and their genetic relation with those isolated in other areas, we investigated the genetic diversity of the 129 CV-A16 strains associated with HFMD epidemics in Fukushima, Japan, from 1983 to 2003, and compared their genetic relation to 49 CV-A16 strains isolated in other areas of Japan and in China by using phylogenetic analysis based on the VP4 sequences. Phylogenetic reconstruction of the CV-A16 strains isolated in Fukushima from 1983 to 2003 demonstrated three distinct genetically divergent clusters related to HFMD epidemics that occurred from 1984 to 1994 (including the 1985 and 1991 outbreaks), HFMD epidemics from 1987 to 1998 (including the 1988 and 1998 outbreaks), and HFMD epidemics from 1995 to 2003 (including the 1995 and 2002 outbreaks). CV-A16 strains isolated during each period in Fukushima formed a single cluster with those isolated during essentially the same time period in other areas of Japan and in China. Our results demonstrated that prevalent CV-A16 strains causing HFMD in Fukushima, Japan, genetically changed twice during 21 epidemics, and changes were also observed in the CV-A16 strains causing HFMD epidemics in other areas. We concluded that repeated outbreaks of CV-A16-related HFMD in Japan were caused, in part, by the introduction of genetically changed CV-A16 strains, which might be transmitted overseas.

Coxsackievirus A16 (CV-A16) and human enterovirus 71 (HEV71) are both major etiologic agents of hand, foot, and mouth disease (HFMD). The surveillance data indicate that CV-A16 and HEV71 infections independently cause large outbreaks and then become quiescent for a period of a few years (6).

HEV71-related illness is more severe, with a significantly greater frequency of serious complications and fatality, than illness caused by CV-A16 (2). In 1997, deaths associated with epidemics of HEV71-associated HFMD in Sarawak, Malaysia, followed by outbreaks with high mortality in Taiwan in 1998 and 2000, raised considerable public concern about the virulence of this virus. Since then, several groups have attempted to describe the molecular epidemiology of HEV71 in the Asia-Pacific region and have reported the relationships of HEV71 epidemics with the genetic diversity of HEV71 strains (1, 5, 10). The results indicate that HEV71 strains causing HFMD outbreaks were genetically changed.

On the other hand, the molecular epidemiology of CV-A16 associated with HFMD epidemics has not been fully described (9). In the present study, we evaluated the relationship between the chronologic CV-A16 epidemics in a restricted area, i.e., Fukushima Prefecture, Japan, and the genetic diversity of the CV-A16 strains. We also examined the geographic genetic relationship between the CV-A16 strains isolated in Fukushima and those isolated in other areas of Japan and China, using phylogenetic analyses constructed using the neighbor-joining method on the basis of the VP4 and VP1 sequences.

MATERIALS AND METHODS

Virus strains. Pharyngeal swab samples were collected from patients with HFMD in the Fukushima Prefecture for virus surveillance and transferred to the Fukushima Institute for Public Health for virus isolation. HEp-2, Vero, and RD-18 cells were used for the isolation of enteroviruses. Confluent cell cultures were seeded in microplate wells and inoculated with 100 μl of maintenance medium and 50 μl of pharyngeal swab samples. The cell cultures were then incubated at 34°C in 5% CO_2–95% air and observed for 7 days to check for cytopathic effects. A blind passage was performed once if no cytopathic effect was observed by the end of the observation period. Virus isolates were identified by a neutralization test using anti-CV-A16 polyclonal antibodies provided from the National Institute of Infectious Diseases in Japan. A total of 322 CV-A16 strains were isolated and identified from 1983 to 2003. Those isolates were stored at −80°C.

PCR and sequence determination of VP4 gene. Randomly selected isolates (63 of 241 strains) from 1983 to 1999 and all isolates (69 strains) from 2000 to 2003 were used for further genetic analysis. A total of 132 strains were isolated from patients with HFMD. The methods of molecular diagnosis of enteroviruses by nested reverse transcription-PCR (RT-PCR) and phylogeny-based classification using the VP4 sequences are described elsewhere (7). Briefly, viral RNA was directly extracted from 100 μl of the stock virus samples using the Smitest R kit (Genome Science Laboratories) according to the manufacturer's instructions. The RNA was dissolved with 10 μl of RNase-free distilled water containing 40 U of RNase inhibitor (RNasin; Promega) and 50 pmol of a reverse primer, OL68-1 [nucleotides (nt) 1178 to 1197, 5′-GGTAA(C/T)TTCCACCACCA(A/G/C/T)CC-3′]. The positions of the primers for RT-PCR were numbered according to the complete nucleotide sequence of the attenuated poliovirus Sabin 1 strain (11). The RNA was subjected to heat denaturation for 15 s at 100°C, followed by snap-cooling in an ice-water bath. Reaction mixture (10 μl; 200 U of Moloney murine leukemia virus reverse transcriptase [Life Technology], 2.5 mM deoxynucleoside triphosphates, and 40 U of RNasin [Promega]) was added to each RNA sample. cDNA synthesis was performed for 1 h at 37°C. In total, 5 μl of the

* Corresponding author. Mailing address: Department of Pediatrics, Fukushima Medical University School of Medicine, Hikarigaoka 1, Fukushima 960-1295, Japan. Phone: 81-24-547-1111. Fax: 81-24-548-6578. E-mail: mhosoya@fmu.ac.jp.

▽ Published ahead of print on 8 November 2006.

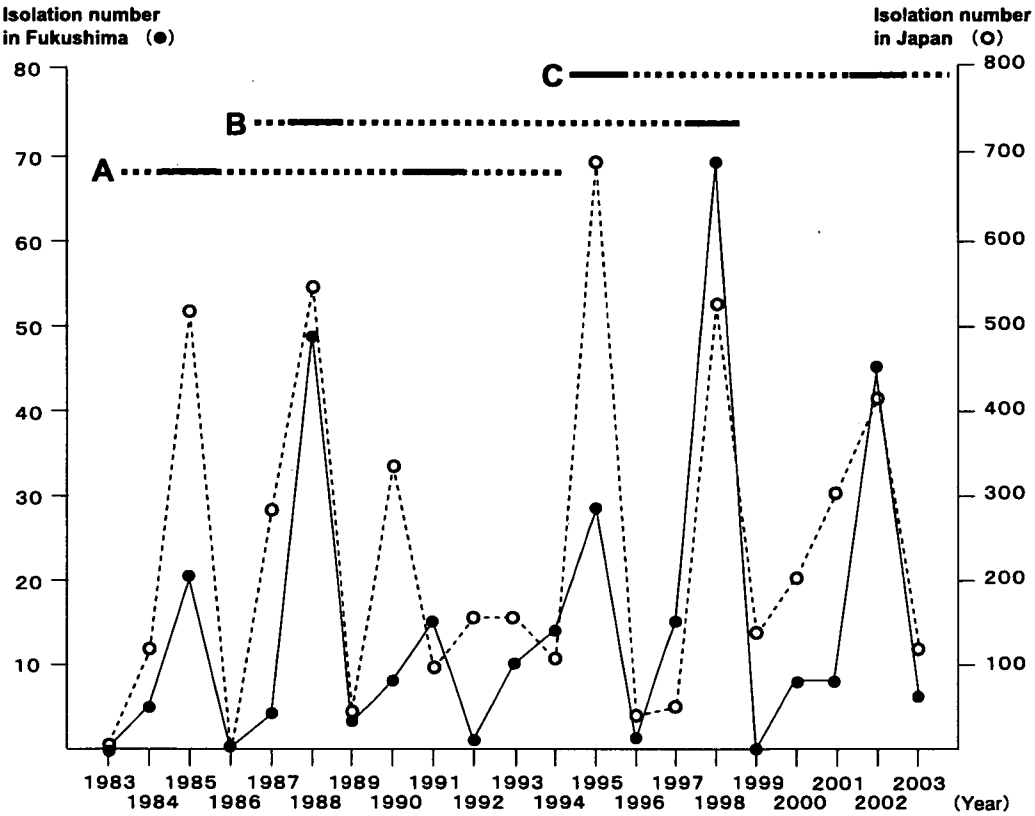

FIG. 1. Numbers of CV-A16 isolates in Fukushima Prefecture and in Japan between 1983 and 2003. Numbers of CV-A16 isolates in Fukushima (closed circles and solid line) and in Japan (open circles and broken line) are expressed, as reported to the Infectious Disease Surveillance Center in Japan by prefectural and municipal public health institutes through the Japanese infectious agents surveillance program. A, B, and C refer to genogroups designated based on phylogenetic analysis of the VP4 sequences of CV-A16 strains. Solid bars and broken bars indicate HFMD outbreaks and epidemic periods, respectively, due to corresponding genogroups.

cDNA reaction mixture was added to 45 μl of 1× *Taq* buffer containing 12.5 pmol of a forward primer, MD91 (nt 444 to 468, 5′-CCTCCGGCCCCTGAAT GCGGCTAAT-3′) and 2.5 U of *Taq* DNA polymerase (Roche Diagnostic Systems). Seminested PCR was performed using 5 μl of the PCR product with a pair of primers, EVP4 (nt 541 to 560, 5′-CTACTTTGGGTGTCCGTGTT-3′) and OL68-1. After initial denaturation at 94°C for 5 min, 40 cycles of amplification were performed by using the GeneAmp PCR System 9600 (PE-Applied Biosystems). Each cycle consisted of denaturation at 95°C for 30 s, primer annealing at 55°C for 30 s, and an extension reaction at 72°C for 1 min. The 40 amplification cycles were followed by a final extension at 72°C for 7 min. The first PCR primer pair allowed for amplification of 753 bp, and the seminested PCR primer pair allowed for amplification of 656 bp. The final PCR products encoded the 3′ one-third of the 5′ nontranslated region, the entire VP4, and the 5′ one-third of VP2 of each CV-A16 strain. The PCR products, including the entire VP4 sequences, were separated in 1% agarose gels and purified with a QIAquick gel extraction kit (QIAGEN). The nucleotide sequence was determined by using a 373A DNA autosequencer (PE-Applied Biosystems) with fluorescent dideoxy chain terminations (PE-Applied Biosystems) and EVP4 and OL68-1 primers.

Phylogenetic analysis based on the VP4 gene. The entire VP4 nucleotide sequences of the 129 strains isolated in Fukushima were determined and used for phylogeny-based analysis, along with those of 64 prototype enterovirus strains. We estimated the evolutionary distances using the Kimura two-parameter method (8) and constructed unrooted phylogenetic trees with the neighbor-joining method (14). Bootstrap analysis was performed by resampling the data sets 1,000 times. Bootstrap values greater than 70% were considered to be statistically significant for the grouping. The VP4 sequences of representative 54 CV-A16 strains isolated in Fukushima were also compared to those of 20 strains isolated in other areas of Japan, 29 strains in China, and 1 strain in the United Kingdom taken from international databases (GenBank) by using phylogenetic analysis.

PCR and phylogenetic analysis based on the VP1 gene. To confirm the relevance of genogrouping based on the VP4 region, we used the phylogeny-based classification methods using the VP1 sequences that were reported by Oberste et al. (12). Twenty-five CV-A16 strains isolated in Fukushima were randomly selected, and their VP1 regions were amplified using two sets of primer pairs, i.e., 055/VP3-011/2A and 055/VP3-009/2A. The VP1 sequences were determined and compared by using phylogenetic analysis with those of 28 strains isolated in China and 1 Taiwan strain taken from international databases.

RESULTS

Chronologic genetic diversity. Enterovirus surveillance data in the Fukushima Prefecture for the period from 1983 to 2003 indicate that peaks of CV-A16 isolations from HFMD occurred in 1985, 1988, 1991, 1995, 1998, and 2002. This epidemic pattern is very similar to that observed in Japanese national surveillance data (Fig. 1) (6). A total of 322 CV-A16 strains were isolated and identified during this period in the Fukushima Prefecture. A nested RT-PCR assay was performed for the detection of enteroviral genome sequences in 63 randomly selected samples collected from 1983 to 1999 and in the 69 samples collected from 2000 to 2003. A positive PCR result was obtained in 129 of 132 samples, and all detected enteroviruses were identified as CV-A16 using PCR-based analysis. Phylogenetic analysis of the VP4 sequences of 129 CV-A16 strains isolated in Fukushima demonstrated the existence of at

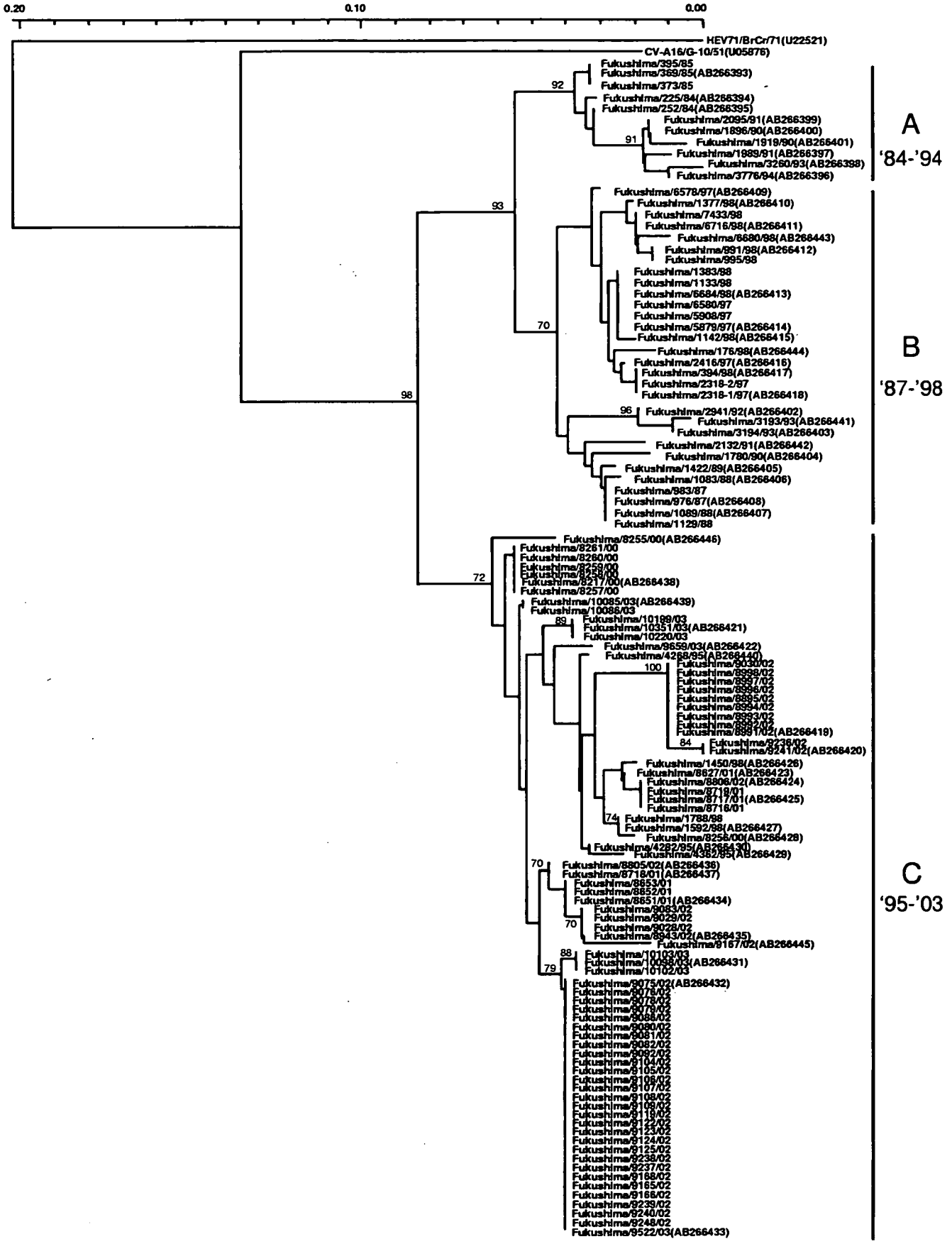
0.20
0.10
0.00
HEV71/BrCr/71(U22521)
CV-A16/G-10/51(U05876)
Fukushima/395/85
Fukushima/369/85(AB266393)
Fukushima/373/85
Fukushima/225/84(AB266394)
Fukushima/252/84(AB266395)
Fukushima/2095/91(AB266399)
Fukushima/1896/90(AB266400)
Fukushima/1919/90(AB266401)
Fukushima/1989/91(AB266397)
Fukushima/3260/93(AB266398)
Fukushima/3776/94(AB266396)
Fukushima/6578/97(AB266409)
Fukushima/1377/98(AB266410)
Fukushima/7433/98
Fukushima/6716/98(AB266411)
Fukushima/6680/98(AB266443)
Fukushima/991/98(AB266412)
Fukushima/995/98
Fukushima/1383/98
Fukushima/1133/98
Fukushima/6684/98(AB266413)
Fukushima/6580/97
Fukushima/5908/97
Fukushima/5879/97(AB266414)
Fukushima/1142/98(AB266415)
Fukushima/176/98(AB266444)
Fukushima/2416/97(AB266416)
Fukushima/394/98(AB266417)
Fukushima/2318-2/97
Fukushima/2318-1/97(AB266418)
Fukushima/2941/92(AB266402)
Fukushima/3193/93(AB266441)
Fukushima/3194/93(AB266403)
Fukushima/2132/91(AB266442)
Fukushima/1780/90(AB266404)
Fukushima/1422/89(AB266405)
Fukushima/1083/88(AB266406)
Fukushima/983/87
Fukushima/976/87(AB266408)
Fukushima/1089/88(AB266407)
Fukushima/1129/88
Fukushima/8255/00(AB266446)
Fukushima/8261/00
Fukushima/8260/00
Fukushima/8259/00
Fukushima/8258/00
Fukushima/8217/00(AB266438)
Fukushima/8257/00
Fukushima/10085/03(AB266439)
Fukushima/10086/03
Fukushima/10199/03
Fukushima/10351/03(AB266421)
Fukushima/10220/03
Fukushima/9659/03(AB266422)
Fukushima/4288/95(AB266440)
Fukushima/9030/02
Fukushima/8999/02
Fukushima/8997/02
Fukushima/8996/02
Fukushima/8895/02
Fukushima/8994/02
Fukushima/8993/02
Fukushima/8992/02
Fukushima/8991/02(AB266419)
Fukushima/9236/02
Fukushima/9241/02(AB266420)
Fukushima/1450/98(AB266426)
Fukushima/8627/01(AB266423)
Fukushima/8806/02(AB266424)
Fukushima/8719/01
Fukushima/8717/01(AB266425)
Fukushima/8716/01
Fukushima/1788/98
Fukushima/1592/98(AB266427)
Fukushima/8258/00(AB266428)
Fukushima/4282/95(AB266430)
Fukushima/4362/95(AB266429)
Fukushima/8805/02(AB266436)
Fukushima/8718/01(AB266437)
Fukushima/8853/01
Fukushima/8852/01
Fukushima/8851/01(AB266434)
Fukushima/9083/02
Fukushima/9029/02
Fukushima/9028/02
Fukushima/8943/02(AB266435)
Fukushima/9167/02(AB266445)
Fukushima/10103/03
Fukushima/10088/03(AB266431)
Fukushima/10102/03
Fukushima/9075/02(AB266432)
Fukushima/9076/02
Fukushima/9077/02
Fukushima/9078/02
Fukushima/9079/02
Fukushima/9088/02
Fukushima/9080/02
Fukushima/9081/02
Fukushima/9082/02
Fukushima/9092/02
Fukushima/9104/02
Fukushima/9105/02
Fukushima/9106/02
Fukushima/9107/02
Fukushima/9108/02
Fukushima/9109/02
Fukushima/9119/02
Fukushima/9122/02
Fukushima/9123/02
Fukushima/9124/02
Fukushima/9125/02
Fukushima/9238/02
Fukushima/9237/02
Fukushima/9168/02
Fukushima/9165/02
Fukushima/9166/02
Fukushima/9239/02
Fukushima/9240/02
Fukushima/9248/02
Fukushima/9522/03(AB266433)
92
91
93
70
98
96
72
89
100
84
74
70
70
88
79
A
'84-'94
B
'87-'98
C
'95-'03

least three genetically distinct groups (bootstrap value of >70%) relating to the epidemics that occurred from 1984 to 1994, from 1987 to 1998, and from 1995 to 2003 (Fig. 2). These three groups were designated genogroups A, B, and C, respectively. The outbreaks in 1985 and 1991 were due to genogroup A, those in 1988 and 1998 were due to genogroup B, and those in 1995 and 2002 were due to genogroup C (Fig. 1). All isolates in Fukushima since 2000 were of genogroup C. CV-A16 strains within a genogroup were slightly genetically divergent in several epidemics.

Geographic genetic relationship. VP4 sequences of representative 54 CV-A16 strains isolated in Fukushima were compared to those of 50 strains taken from international databases (GenBank), which included 20 strains isolated in Japan, 29 strains in China, and 1 United Kingdom strain. Genogroup A strains included 11 CV-A16 strains isolated in Fukushima from 1984 to 1994 and 1 strain isolated in another part of Japan in 1986. Genogroup B strains included 30 CV-A16 strains isolated in Fukushima from 1987 to 1998, 6 strains isolated in other parts of Japan from 1979 to 1998, and 3 strains isolated in Asia from 1999 to 2000. Genogroup C strains included 88 CV-A16 strains isolated in Fukushima from 1995 to 2003, 11 strains isolated in other parts of Japan from 1998 to 2002, 26 strains isolated in Asia from 1998 to 2003, and 1 United Kingdom strain in 1999. In general, each genogroup relating to the epidemics from 1984 to 1994, from 1987 to1998, or from 1995 to 2003 in Fukushima formed a single cluster with CV-A16 strains isolated during almost the same time period in other areas of Japan and in China (Fig. 3). Although the clustering seemed to be more closely related to the period of isolation rather than the area of isolation, the VP4 sequences of strains isolated in Japan were not identical to those isolated in China during the same time period. The GenBank accession numbers of the nucleotide sequences of 54 representative CV-A16 isolates in Fukushima are AB266393 to AB266446. These are indicated in parentheses in Fig. 3, as well as 50 additional strains taken from GenBank.

To clarify whether the genetic diversity occurred as clusters in the VP4 gene or scattered across the gene, the entire VP4 nucleotide sequences of all strains were aligned (Fig. 4). Common genetic diversities were observed in each genogroup. They did not form clusters but appeared randomly throughout the VP4 gene.

Phylogenetic analysis based on the VP1 gene. To confirm the relevance of genogrouping based on the VP4 region, bootstrap analysis was performed using VP1 sequences of 25 CV-A16 strains isolated in Fukushima and 29 strains isolated in other countries. The analysis based on the VP1 gene revealed three genetically distinct groups, and the grouping was completely identical to the results based on the VP4 gene (data not shown). Bootstrap values for the grouping of A, B, and C based on the VP1 gene were 97, 81, and 100%, respectively, and were higher than those based on the VP4 gene (90, 39, and 71%, respectively).

DISCUSSION

CV-A16 causes large outbreaks of HFMD worldwide. Enterovirus surveillance data in the Fukushima Prefecture for the period from 1983 to 2003 indicate that the annual proportion of CV-A16 isolates relative to total enterovirus isolates fluctuated widely, from 0% in 1983, 1986, and 1999 to 35.3% in 2002. Peaks of CV-A16 isolations from HFMD occurred in the years 1985, 1988, 1991, 1995, 1998, and 2002 (6). This epidemic pattern is very similar to that observed in the Japanese national surveillance data (Fig. 1) (6). These observations indicate that CV-A16 follows an epidemic mode of transmission, causing large outbreaks and then becoming quiescent for a period of a few years. Similar quiescence between outbreaks is observed in the meningitis epidemics caused by echovirus type 30. The quiescence is probably due to the development of population immunity that occurs during a high-infection-rate epidemic. The virus might cause only sporadic cases until a large cohort of nonimmune individuals has developed, often over a period of several years, setting the stage for another large epidemic (12).

Phylogeny-based classification using the VP4 sequence is useful for the identification of human enteroviruses (3, 4). The method takes advantage of the detection of the divergence in VP4 sequences both between and within serotypes, and thus is also of use for global epidemiologic studies of enteroviruses (1, 5, 7). We investigated the genetic diversity of CV-A16 strains associated with HFMD epidemics in the Fukushima Prefecture, Japan, from 1983 to 2003 and compared their genetic relation to those isolated in other areas of Japan and in China using the same method. CV-A16 strains isolated in Fukushima, from 1983 to 2003, made at least three distinct clusters on the phylogenetic tree. The three clusters were designated genogroups A, B, and C and were associated with the HFMD epidemics from 1984 to 1994 (including the 1985 and 1991 outbreaks), 1987 to 1998 (including the 1988 and 1998 outbreaks), and 1995 to 2003 (including the 1995 and 2002 outbreaks), respectively. The predominant genogroup was replaced with a new genogroup. CV-A16 strains within a genogroup gradually became genetically divergent in several epidemics. These results demonstrated that the introduction of a new genogroup in addition to the genetic divergence within a genogroup resulted in repeated HFMD outbreaks in Fukushima, Japan.

Each genogroup formed the same cluster with CV-A16 strains isolated during essentially the same time period in other areas of Japan and in China. The clustering seemed to be more closely related to the date of isolation than to the geographic location. Genetic diversities appeared randomly throughout

FIG. 2. Phylogram depicting the phylogenetic relationships on the basis of the VP4 sequence among 129 CV-A16 strains isolated in Fukushima from 1983 to 2003. Bootstrap analysis was performed by resampling the data sets 1,000 times. Bootstrap values greater than 70% were considered to be statistically significant for the grouping and were denoted in the figure. Isolated place, strain name, and isolated year were indicated. The GenBank accession number of one isolate to represent isolates with identical sequences is also indicated in parenthesis. CA-A16/G-10/51 is the prototype CV-A16 strain. The VP4 nucleotide sequence of prototype HEV71/BrCr/71 was used as an outgroup in the analysis.

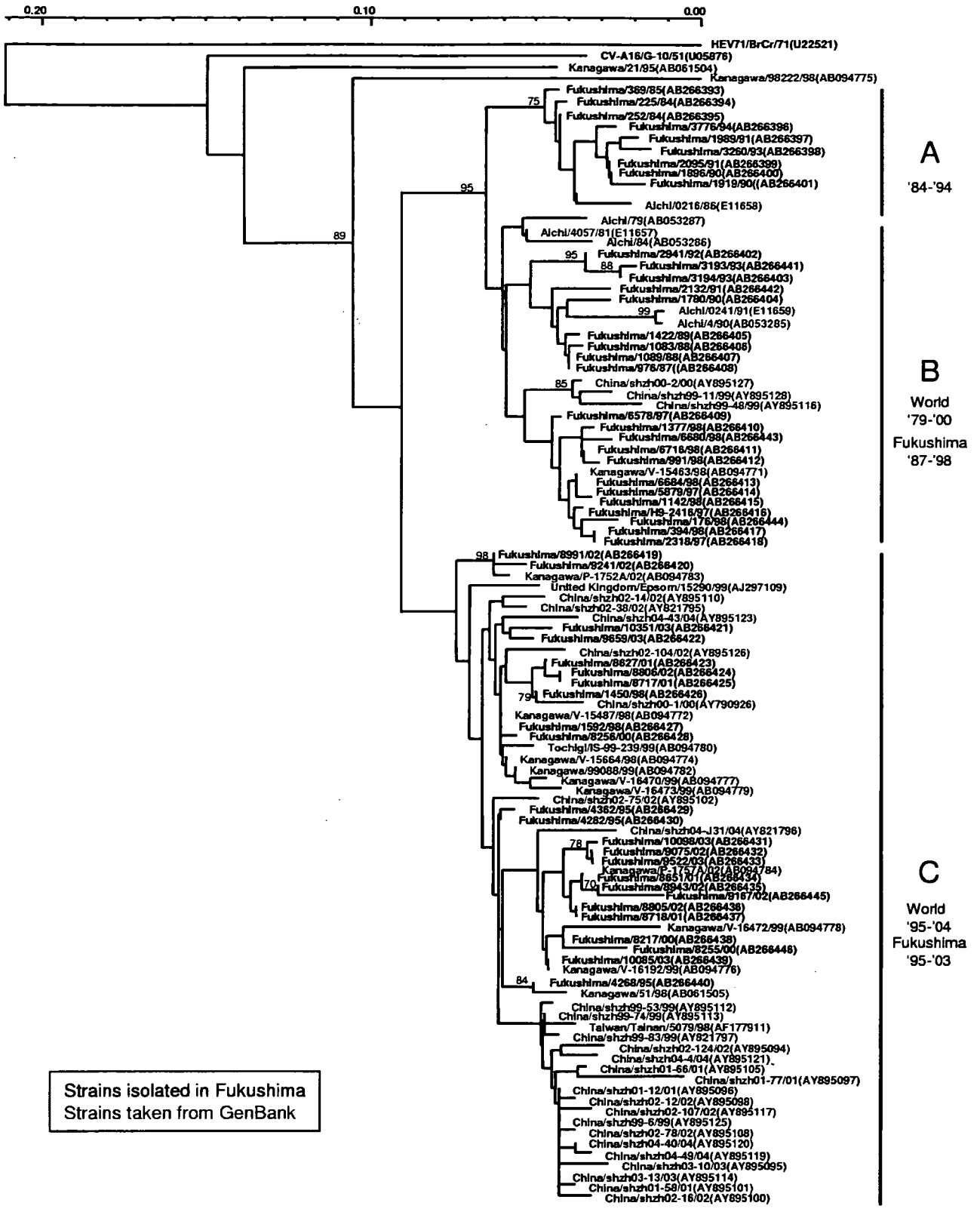

FIG. 3. Phylogram depicting the phylogenetic relationships on the basis of the VP4 sequence among representative 54 CV-A16 strains isolated in Fukushima and 50 CV-A16 strains isolated in Japan, China, and United Kingdom taken from international databases (GenBank). Bootstrap analysis was performed by resampling the data sets 1,000 times. Bootstrap values greater than 70% were considered to be statistically significant for the grouping and were denoted in the figure. Isolated place, strain name, and isolated year were indicated. GenBank accession numbers of CV-A16 strains isolated in Fukushima and the strains taken from international databases are indicated in parentheses. CA-A16/G-10/51 is the prototype CV-A16 strain. The VP4 nucleotide sequence of prototype HEV71/BrCr/71 was used as an outgroup in the analysis.

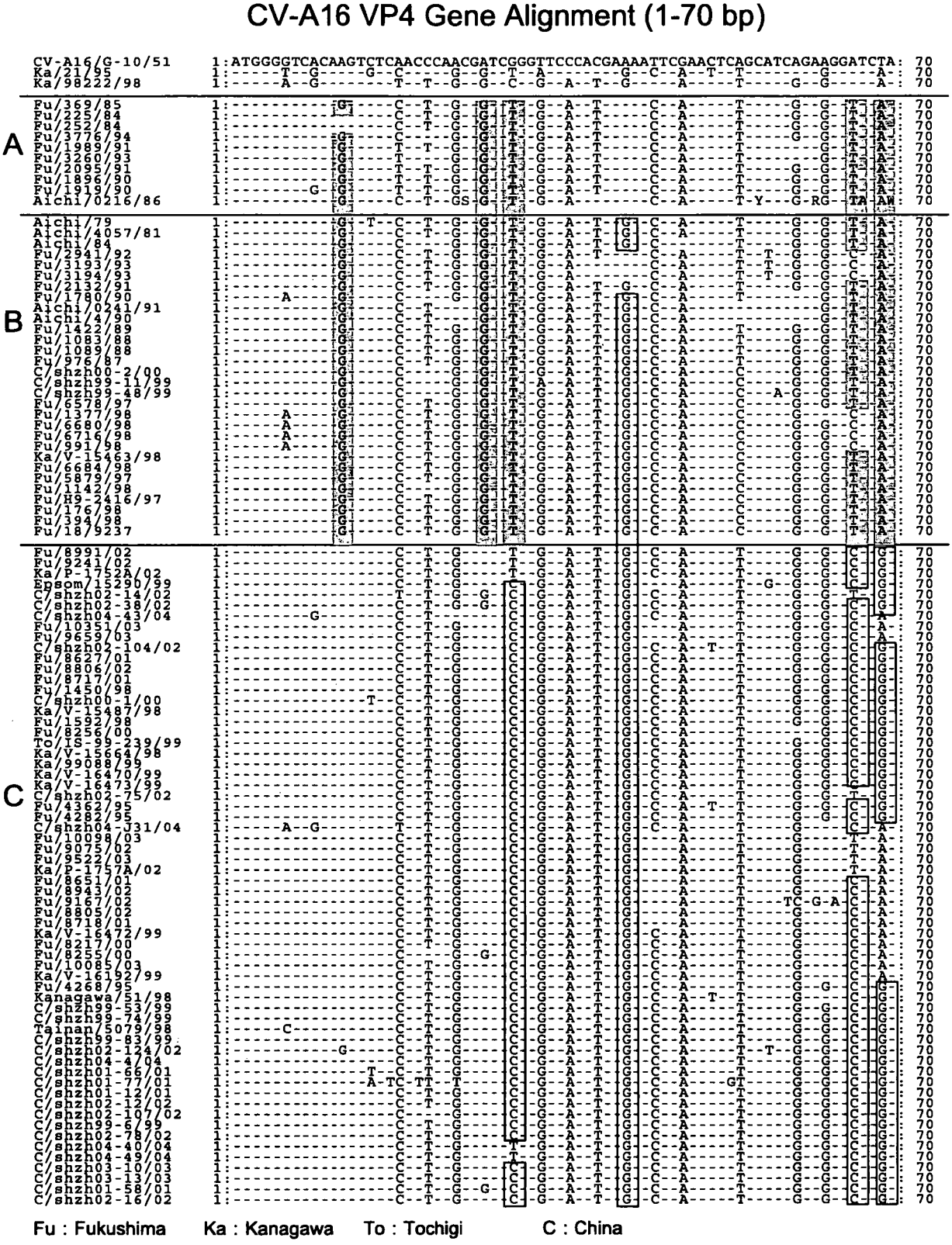

FIG. 4. Alignment of the entire VP4 sequences. Common genetic diversities were observed in each genogroup. Nucleotide differences from the prototype CV-A16/G-10/51 strain observed in genogroup A, genogroup A and B, or genogroup A and C are indicated by shading and those in genogroup B, genogroups B and C, or genogroup C are indicated in boxes.

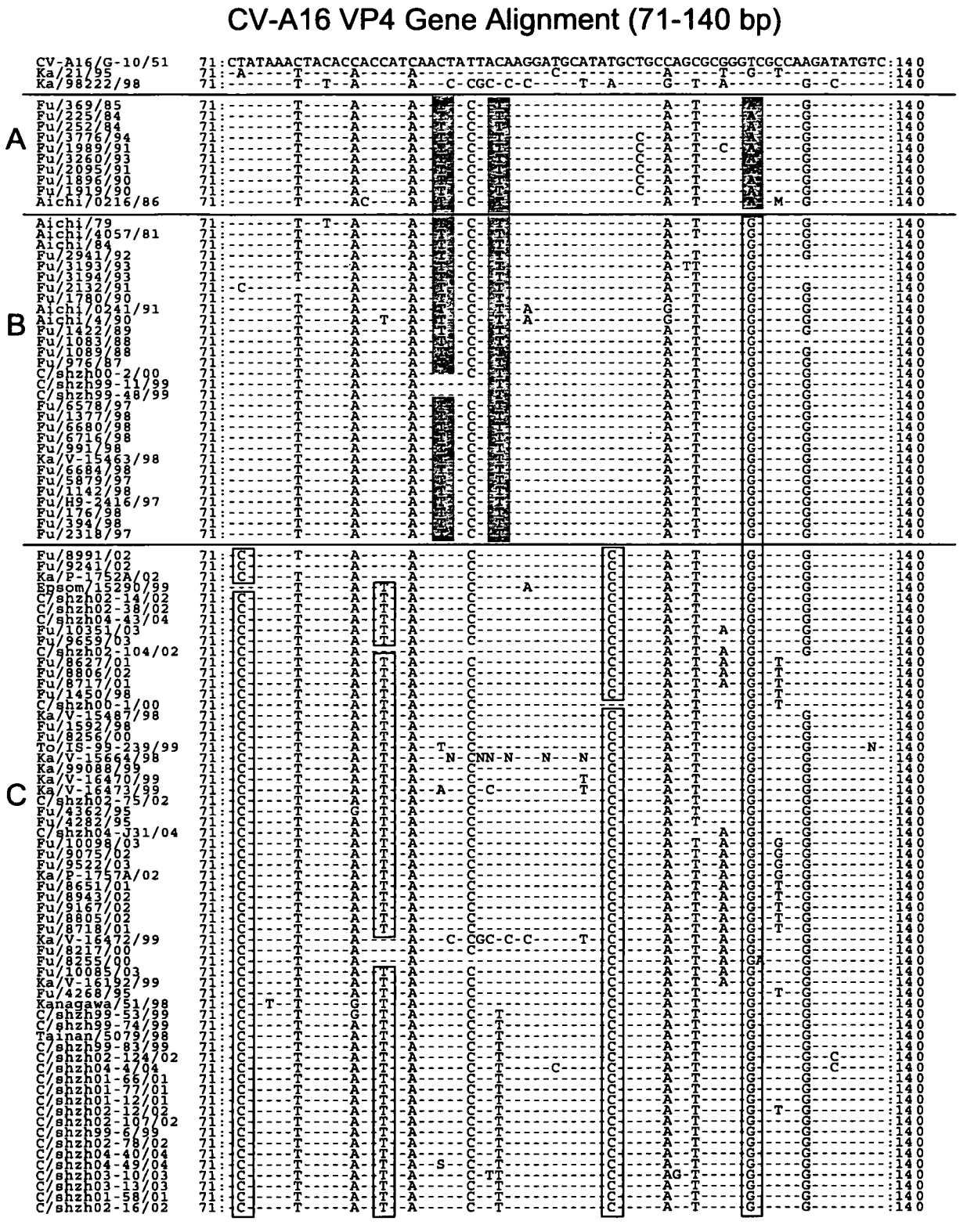

FIG. 4—*Continued.*

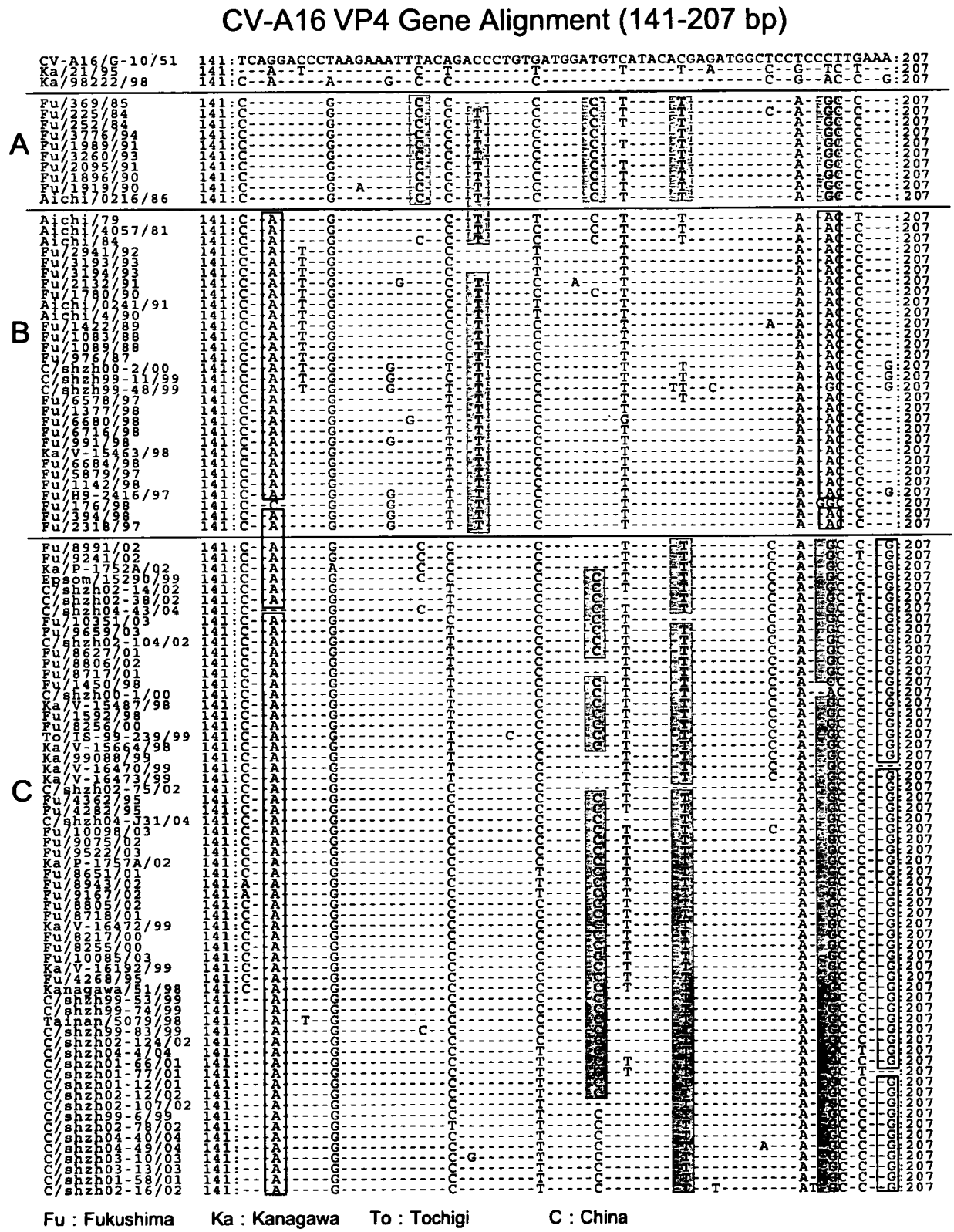

FIG. 4—*Continued.*

the VP4 gene and were common to each genogroup. These indicated that a new CV-A16 genogroup might derive from other regions of the world, be predominant for several years with genetic divergence, and then disappear.

The protein encoded by the VP1 gene is the most exposed and immunodominant of the capsid proteins. Serotypic identification and classification rely on antigenic methods, and VP1 gene sequence data are likely to give the most useful information in molecular epidemiologic studies (13). Shimizu et al. analyzed the phylogeny of HEV71 isolates, which is the other major etiologic agent of HFMD, based on the nucleotide sequence alignment of both the VP1 and VP4 regions (15). Phylogenetic trees based on VP4 sequences revealed that the HEV71 strains isolated from the Western Pacific Region formed two major genogroups, B and C, and were similar to those based on the VP1 sequences. Cardosa et al. reported that the VP1 and VP4 gene sequences both provide similar phylogenetic information, but the higher bootstrap values in the VP1 dendrograms provide greater confidence, particularly when elucidating new genotypes. Thus, the use of the shorter VP4 gene might be helpful for HEV71 surveillance, but the VP1 gene should be used for confirming data obtained with VP4-based analysis (1). Therefore, we confirmed the data obtained from the analysis based on VP4 genes of CV-A16 isolates by using VP1-based analysis. Phylogenetic analysis based on the VP1 gene demonstrated the existence of three genetically distinct groups, and the grouping was completely identical to the result obtained with VP4-based analysis. Bootstrap values for the grouping of A, B, and C based on the VP1 gene were higher than 80%, whereas those for the grouping of A and C based on the VP4 gene were higher than 70%. Although bootstrap values are slightly higher in the VP1 dendrograms than in the VP4 dendrograms, the VP4 gene as well as the VP1 gene seems to be appropriate for the epidemiologic study of CV-A16. In conclusion, phylogenetic analysis based on the VP1 gene confirmed that CV-A16 strains isolated in Fukushima formed three genogroups, and each genogroup formed the same cluster with CV-A16 strains isolated during essentially the same time period in China.

In summary, we describe the evident genetic diversity and changes in the VP4 protein region of CV-A16 strains that were isolated in a restricted region through more than 20 successive epidemics. Our results indicate that CV-A16 strains causing HFMD had genetically changed twice during the period and that these CV-A16 strains might have been transmitted overseas. We conclude that the repeated outbreaks of CV-A16-related HFMD might be caused, in part, by the worldwide transmission of the genetically changed CV-A16 strains, as well as a large cohort of nonimmune individuals. To test this hypothesis, a worldwide surveillance system for HFMD and genetic analysis of isolated CV-A16 strains is necessary.

ACKNOWLEDGMENT

We do not have a commercial or other association that might pose a conflict of interest (e.g., pharmaceutical stock ownership, consultancy, advisory board membership, relevant patents, or research funding).

REFERENCES

1. **Cardosa, M. J., D. Perera, B. A. Brown, D. Cheon, H. M. Chan, K. P. Chan, H. Cho, and P. McMinn.** 2003. Molecular epidemiology of human enterovirus 71 strains and recent outbreaks in the Asia-Pacific region: comparative analysis of the VP1 and VP4 genes. Emerg. Infect. Dis. **9**:461–468.
2. **Chang, L. Y., T. Y. Lin, Y. C. Huang, K. C. Tsao, S. R. Shih, M. L. Kuo, H. C. Ning, P. W. Chung, and C. M. Kang.** 1999. Comparison of enterovirus 71 and coxsackievirus A16 clinical illness during the Taiwan enterovirus epidemic, 1998. Pediatric. Infect. Dis. J. **18**:1092–1096.
3. **Hosoya, M., M. Sato, K. Honzumi, M. Katayose, Y. Kawasaki, H. Sakuma, K. Kato, Y. Shimada, H. Ishiko, and H. Suzuki.** 2001. Association of nonpolio enteroviral infection in the central nervous system of children with febrile seizures. Pediatrics **107**:E12.
4. **Hosoya, M., H. Ishiko, Y. Shimada, K. Honzumi, S. Suzuki, K. Kato, and H. Suzuki.** 2002. Diagnosis of group A coxsackieviral infection using polymerase chain reaction. Arch. Dis. Child. **87**:316–319.
5. **Hosoya, M., Y. Kawasaki, M. Sato, K. Honzumi, A. Kato, T. Hiroshima, H. Ishiko, and H. Suzuki.** 2006. Genetic diversity of enterovirus 71 associated with hand, foot, and mouth disease epidemics in Japan from1983 to 2003. Pediatr. Infect. Dis. J. **25**:691–694.
6. **Infectious Disease Surveillance Center.** 2004. Infectious agents surveillance report: enterovirus isolation from aseptic meningitis cases, 1982–2003, Tokyo, Japan. Infectious Disease Surveillance Center, Tokyo, Japan. (In Japanese.)
7. **Ishiko, H., Y. Shimada, M. Yonaha, O. Hashimoto, A. Hayashi, K. Sakae, and N. Takeda.** 2002. Molecular diagnosis of human enteroviruses by phylogeny-based classification by use of the VP4 sequence. J. Infect. Dis. **185**: 744–754.
8. **Kimura, M.** 1980. A simple method for estimating evolutionary rates of base substitutions through comparative studies of nucleotide sequences. J. Mol. Evol. **16**:111–120.
9. **Li, L., Y. He, H. Yang, J. Zhu, X. Xu, J. Dong, Y. Zhu, and Q. Jin.** 2005. Genetic characteristics of human enterovirus 71 and coxsackievirus A16 circulating from 1999 to 2004 in Shenzhen, People's Republic of China. J. Clin. Microbiol. **43**:3835–3839.
10. **McMinn, P., K. Lindsay, D. Perera, H. M. Chan, K. P. Chan, and M. J. Cardosa.** 2001. Phylogenetic analysis of enterovirus 71 strains isolated during linked epidemics in Malaysia, Singapore, and Western Australia. J. Virol. **75**:7732–7738.
11. **Nomoto, A., T. Omata, H. Toyoda, S. Kuge, H. Horie, Y. Kataoka, Y. Genba, Y. Nakano, and N. Imura.** 1982. Complete nucleotide sequence of the attenuated poliovirus Sabin 1 strain genome. Proc. Natl. Acad. Sci. USA **79**:5793–5797.
12. **Oberste, M. S., K. Maher, M. L. Kennett, J. J. Campbell, M. S. Carpenter, D. Schnurr, and M. A. Pallansch.** 1999. Molecular epidemiology and genetic diversity of echovirus type 30 (E30): genotypes correlate with temporal dynamics of E30 isolation. J. Clin. Microbiol. **37**:3928–3933.
13. **Oberste, M. S., K. Maher, D. A. Kilpatrick, and M. A. Pallansch.** 1999. Molecular evolution of the human enteroviruses: correlation of serotype with VP1 sequence and application to picornavirus classification. J. Virol. **73**:1941–1948.
14. **Saitou, N., and M. Nei.** 1987. The neighbor-joining method: a new method for reconstructing phylogenetic trees. Mol. Biol. Evol. **4**:406–425.
15. **Shimizu, H., A. Utama, N. Onnimala, C. Li, Z. Li-Bi, M. Yu-Jie, Y. Pongsuwanna, and T. Miyamura.** 2004. Molecular epidemiology of enterovirus 71 infection in the Western Pacific region. Pediatr. Int. **46**:231–235.

Clinical and Experimental Allergy, 37, 608–614

ORIGINAL PAPER

Cysteinyl leukotrienes enhance tumour necrosis factor-α-induced matrix metalloproteinase-9 in human monocytes/macrophages

T. Ichiyama, M. Kajimoto, M. Hasegawa, K. Hashimoto, T. Matsubara and S. Furukawa
Department of Pediatrics, Yamaguchi University School of Medicine, Yamaguchi, Japan

Clinical and Experimental Allergy

Summary

Background Matrix metalloproteinase-9 (MMP-9) is an important enzyme responsible for airway remodelling. Monocytes/macrophages have a cysteinyl leukotriene 1 (cysLT1) receptor, but its function is poorly understood.

Objective To elucidate the function of the cysLT1 receptor of human monocytes/macrophages in MMP-9 production.

Methods We examined the effect of cysLTs (LTC4, -D4 and -E4) on TNF-α-induced MMP-9 production in THP-1 cells, a human monocytic leukaemia cell line and peripheral blood $CD14^+$ monocytes/macrophages. In addition, we examined the effect of pranlukast, a cysLT1 receptor antagonist, on the enhancement of TNF-α-induced MMP-9 production by cysLTs.

Results ELISA revealed that LTC4 and -D4, but not -E4, enhanced TNF-α-induced MMP-9 production in THP-1 cells and peripheral blood $CD14^+$ monocytes/macrophages. Real-time polymerase chain reaction demonstrated that LTC4 and -D4, but not -E4, increased MMP-9 mRNA expression induced by TNF-α in THP-1 cells. Moreover, we demonstrated that pranlukast completely inhibited the enhancement of TNF-α-induced MMP-9 production by LTC4 and -D4 in THP-1 cells and peripheral blood $CD14^+$ monocytes/macrophages.

Conclusion LTC4 and -D4 enhanced the TNF-α-induced MMP-9 production via binding the cysLT1 receptor in human monocytes/macrophages. Pranlukast inhibited the enhancements by LTC4 and D4.

Correspondence:
Takashi Ichiyama, Department of Pediatrics, Yamaguchi University School of Medicine, 1-1-1 Minamikogushi, Ube, Yamaguchi 755-8505, Japan.
E-mail: ichiyama@yamaguchi-u.ac.jp

Keywords cysteinyl leukotrienes, matrix metalloproteinase-9, monocytes/macrophages, pranlukast, remodelling
Submitted 4 August 2006; revised 14 January 2007; accepted 8 February 2007

Introduction

Matrix metalloproteinases (MMPs) constitute a family of enzymes that mediate the degradation of extracellular matrix proteins [1]. MMPs play important roles in normal and pathological processes, including embryogenesis, wound healing, inflammation, cardiovascular diseases, pulmonary diseases and cancer [2]. MMP-9 is a member of this family, and is capable of degrading collagen IV, a major component of the basement membrane of airways [3]. The activity of MMPs is further controlled by specific tissue inhibitors of metalloproteinases (TIMPs) [4]. TIMP-1 has a high avidity for MMP-9 [5]. The MMP-9, TIMP-1 and MMP-9/TIMP-1 balance is understood to be related to airway remodelling [6, 7]. A recent study demonstrated that allergen-challenged MMP-9-deficient mice had less peribronchial fibrosis and total lung collagen compared with allergen-challenged wild-type mice [8].

Cysteinyl leukotrienes (cysLTs), such as leukotriene C4 (LTC4), -D4 and -E4, induce contraction of the tracheal muscle and have potent effects on leucocyte trafficking, airway mucus secretion and collagen synthesis [9–12]. Normal peripheral blood leucocytes, such as basophils, eosinophils, B lymphocytes and monocytes/macrophages, have a cysLT1 receptor [13]. However, the function of these cells, especially monocytes/macrophages, is poorly understood.

Alveolar macrophages (AM) are the most abundant cells, not only in the alveoli and distal air spaces but also in the conducting airways [14]. Activated AM in asthma may participate in the inflammatory events associated with allergic disease of the lower airways, including the

release of cytokines, chemokines, arachidonic acid metabolites, products of activated O_2 and by direct interaction with T lymphocytes [15–19].

We examined the effect of cysLTs on the productions of MMP-9 and TIMP-1, and on MMP-9 release by previously reported inducers of MMP-9, including IL-13, IL-17, TGF-β1, TNF-α and lipopolysaccharide (LPS), in human monocytes/macrophages [20–24].

Methods

Cell culture and stimulation conditions

THP-1 cells, a human monocytic leukaemia cell line that has a cysLT1 receptor [25], obtained from the American Type Culture Collection, were maintained at 37 °C under humidified 5% CO_2 as stationary cultures. The cells were grown in RPMI 1640 medium containing 10% fetal bovine serum (FBS), 100 U/mL of penicillin and 100 μg/mL of streptomycin. Peripheral blood mononuclear cells (PBMC) were obtained from heparinized blood from 10 healthy medication-free volunteers, with informed consent, by Histopaque 1077 (Sigma Chemical Co., St Louis, MO, USA) gradient centrifugation and washing. Purification of individual cell subpopulations was achieved with a high magnetic gradient Mini MACS purification system (Miltenyi, Sunnyvale, CA, USA). $CD14^+$ monocytes/macrophages were isolated by depletion of non-monocytes (negative selection) with a Monocyte Isolation Kit II (Miltenyi). The purity of the isolated cells was determined using the respective fluorescein isothiocyanate (FITC)-conjugated monoclonal antibodies (Becton-Dickinson Biosciences, San Diego, CA, USA) and flow cytometric analysis (FACScan; Becton-Dickinson Biosciences).

Cells were exposed to 5 ng/mL of IL-13, 5 ng/mL of IL-17, 10 ng/mL of TGF-β1, 20 ng/mL of TNF-α and 1 ng/mL of LPS (from *Escherichia coli*, 0111:B4) and/or cysLTs (Sigma Chemical Company). The doses were determined in accordance with previous studies that investigated MMP-9-relaease by each mediator [20–24]. Some samples were pretreated with pranlukast, a cysLT1 receptor antagonist, provided by ONO Pharmaceutical Co. (Osaka, Japan) for 30 min before the addition of cysLTs. The supernatant fluid, both before and after the addition of cysLTs, was harvested for the determination of MMP-9 and TIMP-1 levels, and then stored at −20 °C.

Determination of MMP-9 and TIMP-1 concentrations

The concentrations of MMP-9 and TIMP-1 were determined with sandwich-type ELISA kits (Amersham, Buckinghamshire, UK). Assays were performed following the instructions of the manufacturer. The detection limits were 0.125 ng/mL for MMP-9 and 2.4 ng/mL for TIMP-1. The assay of MMP-9 recognizes the pro and active forms of MMP-9.

Real-time reverse transcription polymerase chain reaction

Real-time reverse transcription (RT)-polymerase chain reaction (PCR) was performed to determine the mRNA levels of MMP-9 in the THP-1 cells subjected to the indicated treatments. Total cellular RNA was isolated using the TRIzol reagent (Invitrogen, Leek, the Netherlands) according to the manufacturer's instructions. RT was carried out with 2 μg of total RNA and Random Primers (Invitrogen) in a reaction volume of 20 μL using the SuperScript™ III RTS First-strand Strips System (Invitrogen) following the instructions provided. Real-time PCR was carried out using TaqMan Gene Expression Assays and the ABI PRISM 7900 HT Sequence Detection System (Applied Biosystems, Foster City, CA, USA). The PCRs were recorded in real time and analyzed using the accompanying software, Relative Quantification Program. The mRNA level of the GAPDH housekeeping gene was also determined by real-time RT-PCR in each cDNA sample to normalize the expression of the genes of interest (MMP-9).

Statistical analysis

The values of MMP-9 and TIMP-1 concentrations are expressed as means ± SD. Statistical analysis was performed with the Wilcoxon matched-paired test, with a P-value of < 0.05 considered to be significant.

Results

Figure 1 demonstrates total MMP-9 release by the stimulation of LTC4, IL-13, IL-17, TGF-β1, TNF-α and LPS for 24 h in THP-1 cells. Only TNF-α and LPS induced MMP-9 in THP-1 cells. LTC4 significantly enhanced the MMP-9 production induced by IL-13, IL-17, TGF-β1 and TNF-α, but not by LPS (Fig. 1). The enhancement of TNF-α-induced MMP-9 release by LTC4 was significantly greater than that of IL-13, IL-17 and TGF-β1 ($P < 0.01$ for all). The levels of active MMP-9 were lower than the detection limit in the media of cells treated with any stimulators.

LTC4 and -D4 but not -E4 (10–1000 ng/mL) significantly increased MMP-9 release by TNF-α in THP-1 cells, and the potencies of LTC4 and -D4 for TNF-α-induced MMP-9 production were similar (Fig. 2). The potencies of LTC4 and -D4 were not dose related.

The time course of MMP-9 production was examined by incubating THP-1 cells with TNF-α and 100 ng/mL LTC4 during a 48-h period (Fig. 3). MMP-9 production could be observed 8 h after the addition of TNF-α and LTC4, and gradually increased over 48 h.

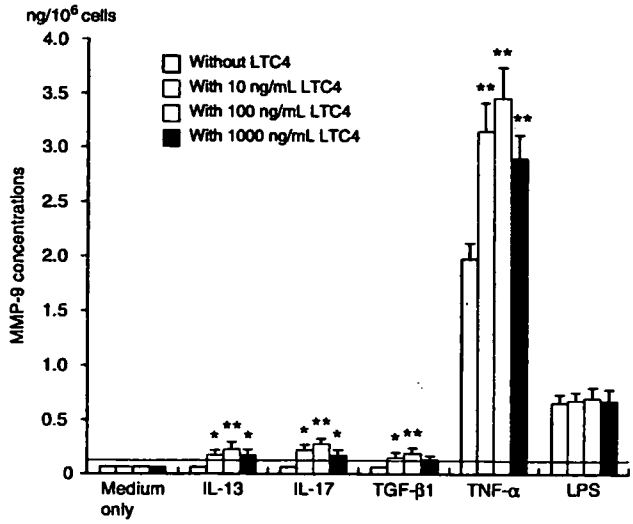

Fig. 1. Matrix metalloproteinase-9 (MMP-9) production, as measured by ELISA, in THP-1 cells stimulated by IL-13, IL-17, TGF-β1, TNF-α or lipopolysaccharide (LPS) with/without LTC4, for 24 h. Data ($n = 8$) are presented as means ± SD. A line indicates the detection limit. $^{**}P < 0.01$ and $^{*}P < 0.05$ compared with cells treated without LTC4.

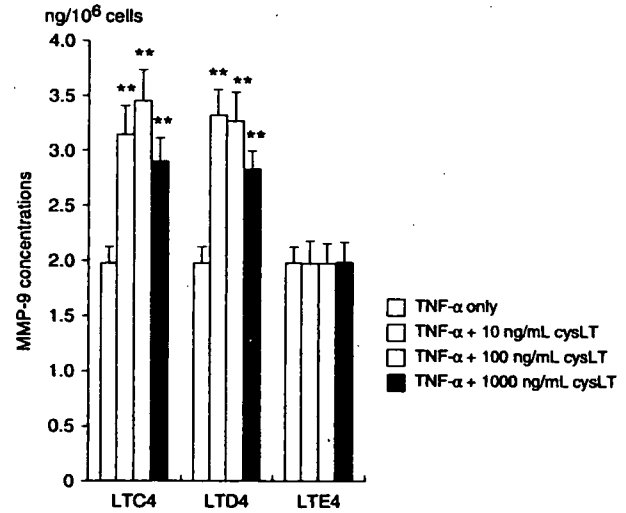

Fig. 2. Matrix metalloproteinase-9 (MMP-9) production, as measured by ELISA, in THP-1 cells stimulated with TNF-α and cysteinyl leukotriene 1 (cysLTs) (LTC4, -D4 or -E4) for 24 h. Data ($n = 8$) are presented as means ± SD. $^{**}P < 0.01$ compared with cells treated with TNF-α only.

ELISA demonstrated that LTC4, IL-13, IL-17, TGF-β1, TNF-α or LPS did not induce TIMP-1 in THP-1 cells (Fig. 4).

The time courses of the inhibitory effects of pretreatments with 10^{-7} M pranlukast on MMP-9 production induced by TNF-α and 100 ng/mL LTC4 were examined in THP-1 cells over 48 h (Fig. 3). Pranlukast blocked MMP-9 production during the experiment. Pranlukast similarly blocked MMP-9 production induced by TNF-α and 100 ng/mL LTD4 during the experiment (data not shown).

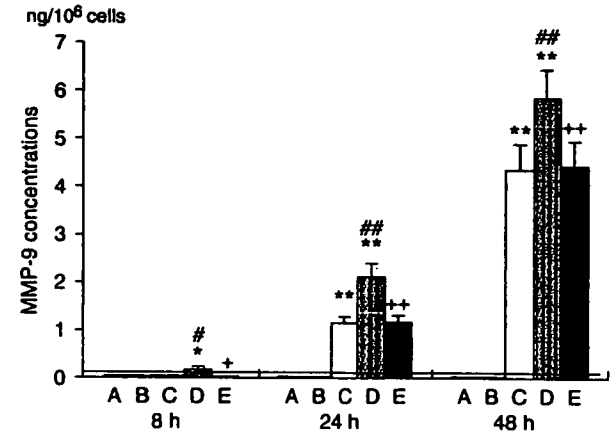

Fig. 3. Kinetics of matrix metalloproteinase-9 (MMP-9) production and the inhibitory effect of pranlukast on MMP-9 release, as measured by ELISA, in THP-1 cells stimulated with LTC4 (B), TNF-α (C) and TNF-α+LTC4 (D) for 8, 24 and 48 h, and cells pretreated with pranlukast for 30 min before TNF-α+LTC4 treatment (E). (A) Cells with no treatment. Data ($n = 8$) are presented as means ± SD. A line indicates the detection limit. $^{**}P < 0.01$ and $^{*}P < 0.05$ compared with cells with no treatment. $^{\#\#}P < 0.01$ and $^{\#}P < 0.05$, compared with cells treated with TNF-α only. $^{++}P < 0.01$, and $^{+}P < 0.05$ compared with cells treated with TNF-α and LTC4.

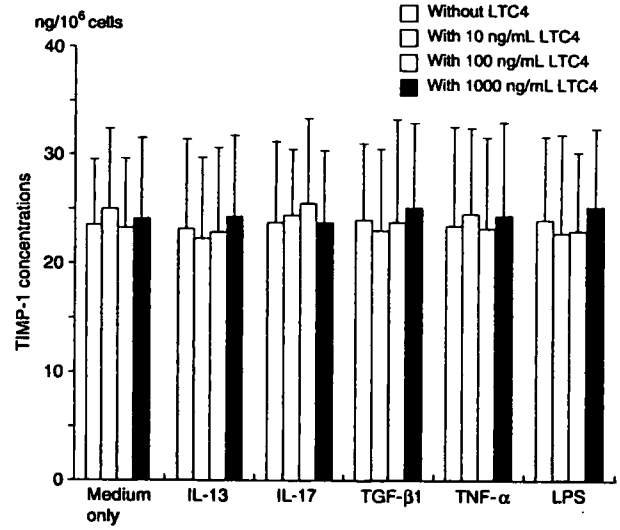

Fig. 4. Tissue inhibitors of metalloproteinases (TIMP)-1 production, as measured by ELISA, in THP-1 cells stimulated by IL-13, IL-17, TGF-β1, TNF-α or lipopolysaccharide (LPS) with/without LTC4, for 24 h. Data ($n = 8$) are presented as means ± SD.

The concentrations of MMP-9 in the culture fluid of THP-1 cells exposed to TNF-α and 100 ng/mL LTC4, -D4 or -E4, in the presence or absence of pranlukast, for 24 h are shown in Fig. 5. The production of MMP-9 induced by TNF-α and cysLTs was significantly inhibited by 10^{-6}–10^{-8} M pranlukast. The effect of pranlukast was dose related.

Real-time PCR demonstrated that MMP-9 mRNA expression was significantly increased 24 h after the

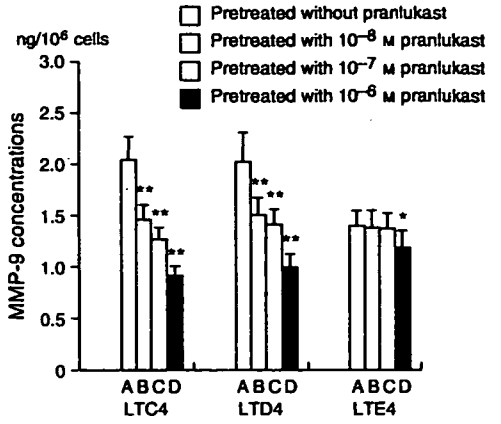

Fig. 5. Inhibitory effect of pranlukast on matrix metalloproteinase-9 (MMP-9) release, as measured by ELISA, in THP-1 cells stimulated with TNF-α and LTC4, -D4 or -E4 for 24 h. The cells were pretreated with pranlukast for 30 min before TNF-α and LTC4, -D4 or -E4 treatments. Cells pretreated without pranlukast (A) Cells pretreated with 10^{-8} (B), 10^{-7} (C) or 10^{-6} M (D) pranlukast. Data ($n = 8$) are presented as means ± SD. $^{**}P < 0.01$ and $^{*}P < 0.05$ compared with cells pretreated without pranlukast.

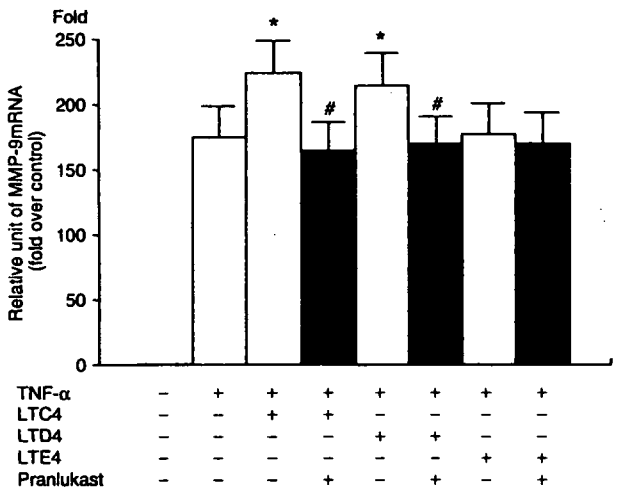

Fig. 6. Matrix metalloproteinase-9 (MMP-9) mRNA expression and the inhibitory effect of pranlukast on MMP-9 mRNA expression, as measured by real-time PCR, in THP-1 cells stimulated with TNF-α and 10^{-6} M LTC4, -D4 or -E4 for 24 h, and cells pretreated with 10^{-7} M pranlukast for 30 min before TNF-α and LTC4, -D4 or -E4 treatments. Data ($n = 8$) are presented as means ± SD. $^{*}P < 0.05$ compared with cells treated with TNF-α only. $^{\#}P < 0.05$ compared with cells treated with TNF-α and LTC4 or -D4.

addition of TNF-α in THP-1 cells ($P < 0.01$) (Fig. 6). Moreover, 100 ng/mL LTC4 and -D4, but not -E4, significantly enhanced the MMP-9 mRNA expression induced by TNF-α (Fig. 6). Pretreatment with 10^{-7} M pranlukast significantly decreased the MMP-9 mRNA expression caused by the stimulation of TNF-α and LTC4, or -D4 in THP-1 cells (Fig. 6).

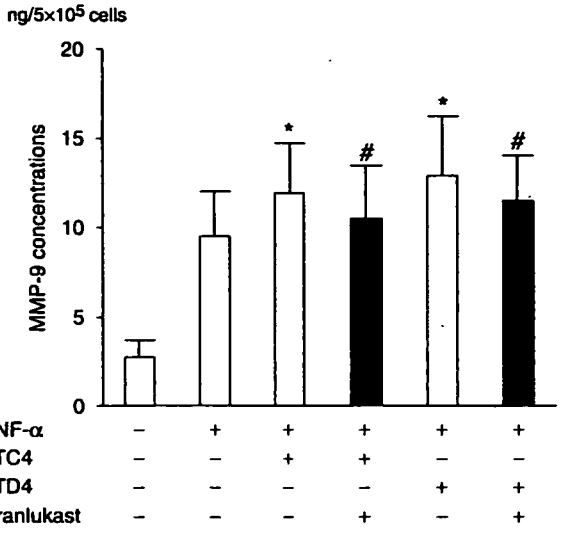

Fig. 7. Inhibitory effect of pranlukast on matrix metalloproteinase-9 (MMP-9) release, as measured by ELISA, in peripheral blood $CD14^+$ monocytes/macrophages stimulated with TNF-α and LTC4 or -D4 for 24 h. The cells were pretreated with pranlukast for 30 min before TNF-α and LTC4 or -D4 treatments. Data ($n = 10$) are presented as means ± SD. $^{*}P < 0.05$ compared with cells treated with TNF-α only. $^{\#}P < 0.05$ compared with cells treated with TNF-α and LTC4 or -D4.

The purity of the $CD14^+$ cells obtained after negative selection with the MACS system was 85.8 ± 6.1%. The MMP-9 production and the inhibitory effect of pranlukast on MMP-9 production were examined by incubating peripheral blood $CD14^+$ monocytes/macrophages with TNF-α and LTC4 or -D4 for 24 h, with some samples being pretreated with 10^{-7} M pranlukast (Fig. 7). LTC4 and -D4 significantly enhanced the MMP-9 production induced by TNF-α in peripheral blood $CD14^+$ monocytes/macrophages ($P < 0.05$). The production of MMP-9 induced by TNF-α and LTC4 or -D4 was significantly inhibited by 10^{-7} M pranlukast ($P < 0.05$).

Discussion

Airway remodelling is an important factor in the pathogenesis of bronchial asthma. MMP-9 is thought to be an important mediator in the airway remodelling of asthma [6, 7, 26–29]. The expressions of MMP-9 in the sputum [26, 30], bronchoalveolar lavage fluid [31] and airway epithelial cells [29, 32] were increased in asthma. In addition, ovalbumin (OVA)-challenged MMP-9-deficient mice have reduced levels of peribronchial fibrosis compared with OVA-challenged wild-type mice [28]. Moreover, MMP-9 induces T cells, neutrophils and eosinophils through the basement membrane [33–35]. It is likely that MMP-9 promotes airway remodelling and inflammation in asthma.

Several recent papers have demonstrated that TNF-α plays a critical role in the initiation and amplification of airway inflammation in asthmatic patients [36–39]. TNF-α induces the adhesion, migration and activation of inflammatory cells, secretion of mucin, apoptosis and the modulation of repair of airway epithelial cells, increased responsiveness of smooth-muscle cells to contractile agents, proliferation and activation of myofibroblasts and fibroblasts and increased synthesis of extracellular matrix glycoproteins [36]. The expression of TNF-α in the airway was related to the severity of asthma [38]. The soluble TNF-α receptor etanercept was beneficial in patients with refractory asthma [39].

Our present study demonstrated that only cysLTs could not increase the expression of MMP-9 in THP-1 cells, but LTC4 and -D4 could enhance TNF-α-induced MMP-9 expression. It is likely that LTC4 and -D4 exert an enhancement of MMP-9 expression induced by TNF-α via the cysLT1 receptor because pranlukast completely blocked the enhancement of TNF-α-induced MMP-9 expression by LTC4 and -D4. The potency of LTC4 and -D4 for TNF-α-induced MMP-9 expression was not dose related. The whole MMP-9 detected in our experiment was the pro form because the levels of active MMP-9 were lower than the detection limit in the media of cells treated with TNF-α in the presence or absence of cysLTs. Ménard and Bissonnette reported that macrophage inflammatory protein-1α (MIP-1α) production induced by 10^{-11} M LTD4 in AM was more than that induced by 10^{-6}, 10^{-8}, 10^{-10}, 10^{-12} or 10^{-14} M LTD4 [14]. We previously reported that monocyte chemoattractant protein-1 (MCP-1) production by cysLTs in human monocytes/macrophages was not dose related [40]. Therefore, it is unlikely that the potency of cysLTs is dose related. Another hypothesis is that higher dosages of LTC4-and -D4 decreased the secretion of MMP-9 because of the potential cell toxicity of LTC4 and -D4 for THP-1 cells. LTD4 would be expected to be about 10 times more potent for calcium flux at the cysLT1 receptors than LTC4 (and 100 times more than LTE4) [41, 42]. The mechanism of enhancement of TNF-α-induced MMP-9 production via cysLT1 receptors of monocytes/macrophages stimulated by cysLTs is different from that of the contraction via cysLT1 receptors of airway smooth muscle stimulated by cysLTs. The potencies of LTC4 and -D4 for the enhancement of TNF-α-induced MMP-9 production in monocytes/macrophages may be different from those for the contraction of airway smooth muscle via the calcium flux.

Pranlukast has some actions in asthma other than as an antagonist of the cysLT1 receptor, including immunomodulation [43]. We have previously demonstrated that pranlukast inhibits the TNF-α-induced nuclear factor-κB (NF-κB) activation [44], and cysLTs-induced MCP-1 production in monocytes/macrophages [40]. In adults administered a single oral dose of 225 mg, Cmax was 642.3 ± 151.0 ng/mL (1.31 ± 0.31 μM) [45], but this value included pranlukast bound to plasma protein. The concentration of free pranlukast was probably less than a tenth of this [46]. Therefore, we think that 10^{-7} and 10^{-8} M pranlukast are clinical doses, and 10^{-6} M is a pharmacological dose. In the animal model, cysLTs promoted airway remodelling in asthma, and the cysLT receptor antagonists inhibited it [10]; however, the mechanism has remained unclear. We revealed one of the mechanisms of airway remodelling associated with cysLTs, and the inhibitory effect of pranlukast. However, the contribution of the anti-remodelling activity of pranlukast at oral therapeutic doses in asthmatic patients remains unclear.

In conclusion, cysLTs enhance TNF-α-induced MMP-9 expression via binding cysLT1 receptor in human monocytes/macrophages *in vitro*, and pranlukast inhibits the enhancement of TNF-α-induced MMP-9 production by cysLTs in the cells.

Acknowledgements

This study was supported by grants from the Ministry of Education, Culture, Sports, Science and Technology (C-17591092), Japan.

References

1 Chandler S, Miller KM, Clements JM *et al.* Matrix metalloproteinases, tumor necrosis factor and multiple sclerosis: an overview. *J Neuroimmunol* 1997; 72:155–61.
2 Chakraborti S, Mandal M, Das S, Mandal A, Chakraborti T. Regulation of matrix metalloproteinases: an overview. *Mol Cell Biochem* 2003; 253:269–85.
3 Nagase H. Activation mechanisms of matrix metalloproteinases. *Biol Chem* 1997; 378:151–60.
4 Murphy G, Knäuper V. Relating matrix metalloproteinase structure to function: why the 'hemopexin' domain? *Matrix Biol* 1997; 15:511–8.
5 Lacraz S, Nicod LP, Chicheportiche R, Welgus HG, Dayer JM. IL-10 inhibits metalloproteinase and stimulates TIMP-1 production in human mononuclear phagocytes. *J Clin Invest* 1995; 96: 2304–10.
6 Atkinson JJ, Senior RM. Matrix metalloproteinase-9 in lung remodeling. *Am J Respir Cell Mol Biol* 2003; 28:12–24.
7 Kelly EA, Jarjour NN. Role of matrix metalloproteinases in asthma. *Curr Opin Pulm Med* 2003; 9:28–33.
8 Lim DH, Cho JY, Miller M, McElwain K, McElwain S, Broide DH. Reduced peribronchial fibrosis in allergen-challenged MMP-9-deficient mice. *Am J Physiol Lung Cell Mol Physiol* 2006; 291:L265–71.
9 Nakai H, Konno M, Kosuge S *et al.* New potent antagonists of leukotrienes C4 and D4. Synthesis and structure-activity relationships. *J Med Chem* 1988; 31:84–91.
10 Henderson WR Jr, Tang LO, Chu SJ *et al.* A role for cysteinyl leukotrienes in airway remodeling in a mouse asthma model. *Am J Respir Crit Care Med* 2002; 165:108–16.

11 Diamant Z, Hiltermann JT, van Rensen EL *et al.* The effect of inhaled leukotriene D4 and methacholine on sputum cell differentials in asthma. *Am J Respir Crit Care Med* 1997; 155: 1247–53.

12 Laitinen LA, Laitinen A, Haahtela T, Vilkka V, Spur BW, Lee TH. Leukotriene E4 and granulocytic infiltration into asthmatic airways. *Lancet* 1993; 341:989–90.

13 Figueroa DJ, Breyer RM, Defoe SK *et al.* Expression of the cysteinyl leukotriene 1 receptor in normal human lung and peripheral blood leukocytes. *Am J Respir Crit Care Med* 2001; 163:226–33.

14 Ménard G, Bissonnette EY. Priming of alveolar macrophages by leukotriene D4: potentiation of inflammation. *Am J Respir Cell Mol Biol* 2000; 23:572–7.

15 Oosterhoff Y, Hoogsteden HC, Rutgers B, Kauffman HF, Postma DS. Lymphocyte and macrophage activation in bronchoalveolar lavage fluid in nocturnal asthma. *Am J Respir Crit Care Med* 1995; 151:75–81.

16 Chanez P, Vignola AM, Lacoste P, Michel FB, Godard P, Bousquet J. Increased expression of adhesion molecules (ICAM-1 and LFA-1) on alveolar macrophages from asthmatic patients. *Allergy* 1993; 48:576–80.

17 Lane SJ, Sousa AR, Lee TH. The role of the macrophage in asthma. *Allergy* 1994; 49:201–9.

18 Tonnel AB, Joseph M, Gosset P, Fournier E, Capron A. Stimulation of alveolar macrophages in asthmatic patients after local provocation test. *Lancet* 1983; 1:1406–8.

19 Viksman MY, Bochner BS, Peebles RS, Schleimer RP, Liu MC. Expression of activation markers on alveolar macrophages in allergic asthmatics after endobronchial or whole-lung allergen challenge. *Clin Immunol* 2002; 104:77–85.

20 Zheng T, Zhu Z, Wang Z *et al.* Inducible targeting of IL-13 to the adult lung causes matrix metalloproteinase- and cathepsin-dependent emphysema. *J Clin Invest* 2000; 106: 1081–93.

21 Prause O, Bozinovski S, Anderson GP, Linden A. Increased matrix metalloproteinase-9 concentration and activity after stimulation with interleukin-17 in mouse airways. *Thorax* 2004; 59:313–7.

22 Duivenvoorden WC, Hirte HW, Singh G. Transforming growth factor β1 acts as an inducer of matrix metalloproteinase expression and activity in human bone-metastasizing cancer cells. *Clin Exp Metastasis* 1999; 17:27–34.

23 Rosenberg GA, Estrada EY, Dencoff JE, Stetler-Stevenson WG. Umor necrosis factor-alpha-induced gelatinase B causes delayed opening of the blood–brain barrier: an expanded therapeutic window. *Brain Res* 1995; 703:151–5.

24 Shankavaram UT, DeWitt DL, Wahl LM. Lipopolysaccharide induction of monocyte matrix metalloproteinases is regulated by the tyrosine phosphorylation of cytosolic phospholipase A2. *J Leukoc Biol* 1998; 64:221–7.

25 Hoshino M, Izumi T, Shimizu T. Leukotriene D4 activates mitogen-activated protein kinase through a protein kinase Cα-Raf-1-dependent pathway in human monocytic leukemia THP-1 cells. *J Biol Chem* 1998; 273:4878–82.

26 Vignola AM, Riccobono L, Mirabella A *et al.* Sputum metalloproteinase-9/tissue inhibitor of metalloproteinase-1 ratio correlates with airflow obstruction in asthma and chronic bronchitis. *Am J Respir Crit Care Med* 1998; 158:1945–50.

27 Hoshino M, Takahashi M, Takai Y, Sim J. Inhaled corticosteroids decrease subepithelial collagen deposition by modulation of the balance between matrix metalloproteinase-9 and tissue inhibitor of metalloproteinase-1 expression in asthma. *J Allergy Clin Immunol* 1999; 104: 356–63.

28 Simpson JL, Scott RJ, Boyle MJ, Gibson PG. Differential proteolytic enzyme activity in eosinophilic and neutrophilic asthma. *Am J Respir Crit Care Med* 2005; 172:559–65.

29 Cho JY, Miller M, McElwain K *et al.* Remodeling associated expression of matrix metalloproteinase 9 but not tissue inhibitor of metalloproteinase 1 in airway epithelium: modulation by immunostimulatory DNA. *J Allergy Clin Immunol* 2006; 117: 618–25.

30 Tanaka H, Miyazaki N, Oashi K, Tanaka S, Ohmichi M, Abe S. Sputum matrix metalloproteinase-9: tissue inhibitor of metalloproteinase-1 ratio in acute asthma. *J Allergy Clin Immunol* 2000; 105:900–5.

31 Lemjabbar H, Gosset P, Lamblin C *et al.* Contribution of 92 kDa gelatinase/type IV collagenase in bronchial inflammation during status asthmaticus. *Am J Respir Crit Care Med* 1999; 159: 1298–307.

32 Hoshino M, Nakamura Y, Sim J, Shimojo J, Isogai S. Bronchial subepithelial fibrosis and expression of matrix metalloproteinase-9 in asthmatic airway inflammation. *J Allergy Clin Immunol* 1998; 102:783–8.

33 Leppert D, Waubant E, Galardy R, Bunnett NW, Hauser SL. T cell gelatinases mediate basement membrane transmigration in vitro. *J Immunol* 1995; 154:4379–89.

34 Delclaux C, Delacourt C, D'Ortho MP, Boyer V, Lafuma C, Harf A. Role of gelatinase B and elastase in human polymorphonuclear neutrophil migration across basement membrane. *Am J Respir Cell Mol Biol* 1996; 14:288–95.

35 Okada S, Kita H, George TJ, Gleich GJ, Leiferman KM. Migration of eosinophils through basement membrane components in vitro: role of matrix metalloproteinase-9. *Am J Respir Cell Mol Biol* 1997; 17:519–28.

36 Erzurum SC. Inhibition of tumor necrosis factor α for refractory asthma. *N Engl J Med* 2006; 357:754–8.

37 Cazzola M, Polosa R. Anti-TNF-α and Th1 cytokine-directed therapies for the treatment of asthma. *Curr Opin Allergy Clin Immunol* 2006; 6:43–50.

38 Howarth PH, Babu KS, Arshad HS *et al.* Tumour necrosis factor (TNF-α) as a novel therapeutic target in symptomatic corticosteroid-dependent asthma. *Thorax* 2005; 60: 1012–8.

39 Berry MA, Hargadon B, Shelley M *et al.* Evidence of a role of tumor necrosis factor α in refractory asthma. *N Engl J Med* 2006; 354:697–708.

40 Ichiyama T, Hasegawa M, Ueno Y, Makata H, Matsubara T, Furukawa S. Cysteinyl leukotrienes induce monocyte chemoattractant protein 1 in human monocytes/macrophages. *Clin Exp Allergy* 2005; 35:1214–9.

41 Evans JF. Cysteinyl leukotriene receptors. *Prostaglandins Other Lipid Mediat* 2002; 68–69:587–97.

42 Capra V. Molecular and functional aspects of human cysteinyl leukotriene receptors. *Pharmacol Res* 2004; 50:1–11.

43 Tohda Y, Nakahara H, Kubo H, Haraguchi R, Fukuoka M, Nakajima S. Effects of ONO-1078 (pranlukast) on

cytokine production in peripheral blood mononuclear cells of patients with bronchial asthma. *Clin Exp Allergy* 1999; 29: 1532–6.

44 Ichiyama T, Hasegawa S, Umeda M, Terai K, Matsubara T, Furukawa S. Pranlukast inhibits NF-κB activation in human monocytes/macrophages and T cells. *Clin Exp Allergy* 2003; 33:802–7.

45 Nakashima M, Kanamaru M, Uematsu T, Tsubokura S. A phase I clinical study of leukotriene C4, D4, and E4 receptor antagonist; ONO-1078 in healthy volunteers. *Rinsho Iyaku* 1993; 9 (Suppl 1):3–29. Japanese.

46 Lynch KR, O'Neill GP, Liu Q *et al.* Characterization of the human cysteinyl leukotriene CysLT1 receptor. *Nature* 1999; 399:789–93.

detected higher incidence rates of occult bacteremia and of IPD overall than were found by community physicians. The baseline incidence rate of IPD in Vancouver (235.7 per 100,000 for 6- to 23-month-old children) was much higher than rates previously reported for urban populations across Canada,[6] which featured in estimations of the cost-effectiveness of PCV7 programs.[9,10] If disease rates were underestimated, the cost-effectiveness of vaccination would have been underestimated as well.

Although this study featured robust case-finding in a large pediatric population, it had some limitations. PCV7 was available for private purchase for 2 years before program implementation, and so the baseline rate of IPD might have been under-estimated. However, no decrease in incidence rates was evident during the 2 preprogram years. The extent of private vaccine use is unknown. Serotype data were lacking for some isolates, and so the rate reduction for serotypes included in the vaccine was estimated rather than directly observed. Immunization histories were missing for some cases. The 2-year observation period after program introduction was likely too short to measure the full impact of vaccination, including indirect protection of other age groups.

We conclude that PCV7 infant vaccination in BC has been highly effective.

REFERENCES

1. Scheifele D, Halperin S, Pelletier L, et al. Invasive pneumococcal infections in Canadian children, 1991–1998: implications for new vaccination strategies. *Clin Infect Dis.* 2000;31:58–64.
2. Poehling KA, LaFleur BJ, Szilagyi PG, et al. Population-based impact of pneumococcal conjugate vaccine in young children. *Pediatrics.* 2004; 114:755–761.
3. Centers for Disease Control. Direct and indirect effects of routine vaccination of children with 7-valent pneumococcal conjugate vaccine on incidence of invasive pneumococcal disease—United States, 1998–2003. *MMWR Morb Mortal Wkly Rep.* 1005;54:893–897.
4. Scheifele DW, Law B, Vaudry W, et al. Invasive pneumococcal infections among Canadian aboriginal children. *Can Commun Dis Rep.* 2003;29:37–42.
5. National Advisory Committee on Immunization. Statement on recommended use of pneumococcal conjugate vaccine. *Can Commun Dis Rep.* 2002;28(ACS-2):1–32.
6. Bjornson GL, Scheifele DW, Halperin SA, et al. Population-based epidemiology of invasive pneumococcal infection in children in nine urban centers in Canada, 1994 through 1998. *Pediatr Infect Dis J.* 2002;21:947–950.
7. Paulus S, David ST, Tang W, et al. Incidence of invasive pneumococcal disease after introduction of the universal infant immunization program, British Columbia (2002–2005). *Can Commun Dis Rep.* 2006;32:157–161.
8. Kellner JD, Church DL, MacDonald J, Tyrrell GJ, Scheifele D. Progress in the prevention of pneumococcal infection. *Can Med Assoc J.* 2005; 173:1149–1151.
9. McClure CA, Ford MW, Wilson JB, Aramini JJ. Expected benefits of pneumococcal vaccination in Canadian infants and children <5 years old. *Can Commun Dis Rep.* 2006;32:45–54.
10. Lebel MH, Kellner JD, Ford-Jones EL, et al. A pharmacoeconomic evaluation of 7-valent pneumococcal conjugate vaccine in Canada. *Clin Infect Dis.* 2003;36:259–268.

MATRIX METALLOPROTEINASE-9 AND TISSUE INHIBITORS OF METALLOPROTEINASES 1 IN INFLUENZA-ASSOCIATED ENCEPHALOPATHY

Takashi Ichiyama, MD, Tsuneo Morishima, MD,† Madoka Kajimoto, MD,* Takeshi Matsushige, MD,* Tomoyo Matsubara, MD,* and Susumu Furukawa, MD**

Abstract: Matrix metalloproteinase-9 (MMP-9) and tissue inhibitors of metalloproteinases 1 (TIMP-1) play important roles in the function of the blood–brain barrier. Serum MMP-9 and TIMP-1 concentrations were determined in influenza virus infection with or without neurologic complications. Our results suggest that an imbalance between MMP-9 and TIMP-1 damages the blood–brain barrier and promotes febrile seizure or encephalopathy in influenza virus infection.

Key Words: Epstein–Barr virus, influenza-associated encephalopathy, MMP-9, respiratory syncytial virus, TIMP-1

Accepted for publication January 19, 2007.

From the *Department of Pediatrics, Yamaguchi University School of Medicine, Yamaguchi, Japan; and the †Department of Pediatrics, Okayama University Graduate School of Medicine and Dentistry, Okayama, Japan.

This study was supported by grants from the Ministry of Health, Labor and Welfare (H18-Shinkou-6) and the Ministry of Education, Culture, Sports, Science and Technology (A-17209037).

Address for correspondence: Takashi Ichiyama, MD, Department of Pediatrics, Yamaguchi University School of Medicine, 1-1-1 Minamikogushi, Ube, Yamaguchi 755-8505, Japan. E-mail: ichiyama@yamaguchi-u.ac.jp.

DOI: 10.1097/INF.0b013e31803994a0

Matrix metalloproteinases (MMPs) constitute a family of zinc-binding proteinases that degrade the extracellular matrix proteins.[1] MMP-9 is mainly produced by inflammatory cells such as T cells and macrophages, and is capable of degrading collagen IV, a major component of the basement membrane of the cerebral epithelium and responsible for the integrity of the blood–brain barrier.[2] The activity of MMPs is further controlled by specific tissue inhibitors of metalloproteinases (TIMPs), and TIMP-1 has a high avidity for MMP-9.[3]

Influenza-associated encephalopathy is a severe neurologic complication of influenza manifesting seizures and progressive coma with a high-grade fever.[4] The pathogenesis of influenza-associated encephalopathy remains unclear. We have reported that several proinflammatory cytokines are elevated in serum and cerebrospinal fluid in patients with influenza-associated encephalopathy and are related to the clinical severity of the disease.[5–8] Brain computed tomography abnormalities, such as brain edema and low densities in localized areas, are associated with a poor prognosis in these patients.[4] A postmortem examination of 1 fatal case of influenza-associated encephalopathy revealed vasogenic brain edema, suggesting that the vascular endothelial cells were impaired.[9] It is possible that the blood–brain barrier is damaged in influenza-associated encephalopathy.

To investigate the role of MMP-9 and TIMP-1 in the pathogenesis of influenza-associated encephalopathy, we determined the relationship between serum concentrations of MMP-9 and TIMP-1 in patients with influenza virus infection with or without neurologic complications.

SUBJECTS AND METHODS

Informed consent was obtained from the parents of the patients and controls enrolled in this study. Serum samples were obtained from influenza-associated encephalopathy patients on admission to Yamaguchi University Hospital and 11 research cooperation hospitals in Japan, from December 1999 to May 2005, and were obtained from the patients with influenza-associated febrile seizures, uncomplicated influenza, Epstein–Barr virus (EBV) infection and respiratory syncytial virus (RSV) infection on admission to Yamaguchi University Hospital from March 2003 to January 2006. The specimens were stored frozen at −80°C until assay.

Influenza-Associated Encephalopathy, Influenza-Associated Febrile Seizures and Uncomplicated Influenza. The criteria for the diagnosis and the day of onset of influenza-associated encephalopathy, influ-

enza-associated febrile seizures and uncomplicated influenza were described in our previous article.[8] Thirty-five patients were enrolled with influenza-associated encephalopathy (22 males and 13 females, aged from 6 months to 19 years: mean, 5.8 years). These patients were divided into 2 groups, ie, those who died (n = 7 of 17) or developed neurologic sequelae (n = 10 of 17), and those who had no sequelae of follow-up (n = 18). Serum samples were obtained from these patients on day 1.0 ± 0.5 (range, 1–3) of the illness.

Thirteen patients were enrolled with influenza-associated febrile seizures (8 males and 5 females, aged from 2 to 10 years: mean, 5.4 years). Serum samples were obtained on day 1.0 ± 0.3 (range, 1–2) of the illness.

Forty-six patients were enrolled with uncomplicated influenza (26 males and 20 females, aged from 11 months to 10 years: mean, 5.2 years), and serum were obtained on days 2.0 ± 1.0 (range, 1–4) of the illness.

Control Subjects. Control subjects comprised 8 patients who had EBV infection (3 males and 5 females, aged from 2 to 12 years: mean, 5.8 years) and 37 patients who had RSV infection (21 males and 16 females, aged from 1 to 19 months: mean, 0.7 years). Serum were obtained from the patients with EBV infection on days 7.0 ± 3.5 (range, 2–13) and those with RSV infection on days 4.0 ± 2.5 (range, 2–7) of the illness. Thirty-three healthy children (15 males and 18 females, aged from 2 to 15 years: mean, 6.4 years) also served as controls.

Determination of MMP-9 and TIMP-1 Concentrations. The serum concentrations of MMP-9 and TIMP-1 were determined with sandwich-type ELISA kits (Amersham, Buckinghamshire, UK). Assays were performed following the manufacturer's instructions. The detection limits were 2.5 ng/mL for MMP-9 and 2.4 ng/mL for TIMP-1.

Statistical Analysis. All values are medians ± SD. The differences in the results between groups were analyzed using the Mann–Whitney *U* test.

RESULTS

Serum MMP-9 concentrations in influenza-associated encephalopathy with poor prognosis, influenza-associated febrile seizures and uncomplicated influenza were significantly higher than the healthy controls ($P < 0.0001$, $P = 0.0005$, $P < 0.0001$, respectively) (Fig. 1). The serum MMP-9 concentrations in influenza-associated encephalopathy with poor prognosis were significantly higher than those for uncomplicated influenza, and the healthy controls ($P = 0.0149$, and $P < 0.0001$, respectively).

Serum TIMP-1 concentrations in influenza-associated encephalopathy with poor prognosis were significantly higher than those in influenza-associated encephalopathy without sequelae, influenza-associated febrile seizures and the healthy controls ($P = 0.0087$, 0.018 and 0.0062, respectively). The serum TIMP-1 concentrations in influenza-associated encephalopathy without sequelae and influenza-associated febrile seizures were significantly lower than those in uncomplicated influenza ($P < 0.0001$ and <0.0001, respectively). The MMP-9/TIMP-1 ratios in influenza-associated encephalopathy with poor prognosis, influenza-associated encephalopathy without sequelae and influenza-associated febrile seizures were significantly higher than those for uncomplicated influenza ($P = 0.0099$, 0.0079 and 0.0053, respectively) and the healthy controls ($P = 0.0134$, 0.012 and 0.0093, respectively).

The serum MMP-9 concentrations and MMP-9/TITMP-1 ratios for uncomplicated influenza were significantly higher than those in EBV infection ($P = 0.0006$ and $P < 0.0001$, respectively) and RSV infection ($P = 0.0002$ and $P < 0.0001$, respectively), and serum TIMP-1 concentrations were significantly lower than those in EBV infection ($P = 0.0001$) and RSV infection ($P = 0.0017$).

DISCUSSION

Results from our present study suggest that MMP-9 and TIMP-1 are related to the pathogenesis of influenza-associated encephalopathy on the basis of the elevated serum MMP-9 and MMP-9/TIMP-1 ratios, and associated with the clinical severity of influenza-associated encephalopathy. The serum MMP-9 levels and MMP-9/TIMP-1 ratios for uncomplicated influenza were significantly higher than those in EBV and RSV infections, and the serum TIMP-1 concentrations for uncomplicated influenza were significantly lower. These findings suggest that TIMP-1 was not sufficiently produced in influenza virus infection compared with RSV and EBV infections, though MMP-9 was abundantly produced in influenza virus infection. However, EBV and RSV infections may be inappropriate disease controls. EBV infection affects lymphocytes, but not airway epithelial cells, and RSV infects young infants. Another hypothesis is that TIMP-1 is overly consumed in influenza virus infection and, as a result, the serum TIMP-1 values are not elevated. In vitro, influenza virus produced MMP-9, but had little effect on TIMP-1, in cultured cells.[10] Moreover, the serum TIMP-1 levels in influenza-associated encephalopathy without sequelae and influenza-associated febrile seizures were significantly lower than those for uncomplicated influenza. One hypothesis is that patients with neurologic complications of influenza could not produce a sufficient amount of TIMP-1. The serum TIMP-1 concentrations in influenza-associated encephalopathy with poor prognosis were not lower than those for the Flu. Interleukin-10 (IL-10) is markedly elevated in the serum of influenza-associated encephalopathy with poor prognosis.[7,8] IL-10 stimulates TIMP-1 production.[3] We hy-

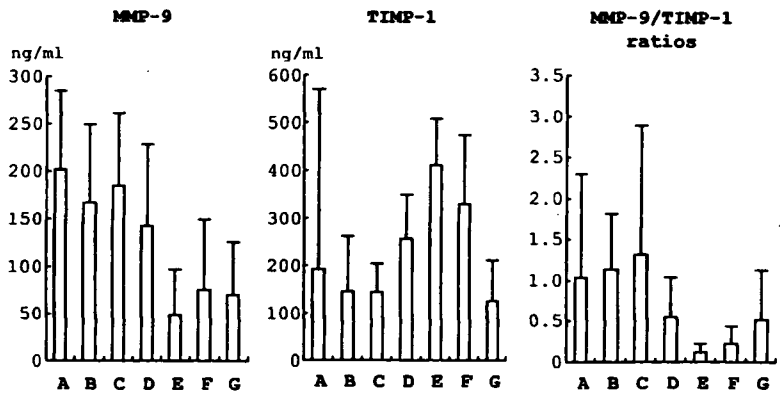

FIGURE 1. Serum concentrations of MMP-9, TIMP-1 and the ratios of MMP-9/TIMP-1 in influenza-associated encephalopathy with poor prognosis (A), influenza-associated encephalopathy without sequelae (B), influenza-associated febrile seizures (C), uncomplicated influenza (D), EBV infection (E), RSV infection (F)and the healthy controls (G). Data are presented as medians + 1 SD.